

Research Paper

Advancing Computational Approaches for Geometry Optimization of Steel Structures¹⁾

Artur LAX, Sławomir MILEWSKI*

*Chair for Computational Engineering, Faculty of Civil Engineering
Cracow University of Technology
Cracow, Poland*

*Corresponding Author e-mail: slawomir.milewski@pk.edu.pl

The primary objective of this study is to develop and assess computational methods for optimizing the geometry of specific building structures modeled through parametric description. The focus is on steel bar structures, including trusses and beams, subjected to varying load conditions with fixed and uncertain parameters. The decision variables in the single- or multi-criteria non-linear optimization problem correspond to selected geometric features of these structures. The proposed methodology revolves around dividing the entire construction into distinct structural patterns. This allows for addressing separate local optimization problems with a reduced number of decision variables, followed by a global optimization considering the interactions between these patterns. This approach is versatile, serving both the design of objects meeting required architectural and structural conditions and constraints, and the optimization of all or specific parameters, incorporating diverse economic (e.g., material usage) and engineering criteria (e.g., limit states).

Keywords: topological optimization; parametric description; deterministic methods; probabilistic methods; steel structures; finite element method.

1. INTRODUCTION

1.1. Motivation

In the design process of steel structures, engineers often grapple with the intricate geometry comprising diverse structural elements that collectively form pertinent systems such as trusses, bracings, and floor beams, among others. These structures present various options in terms of topology, cross-section types, dimensions, and other geometry parameters. Moreover, there is a critical need to establish the structure's geometry at the conceptual design stage,

¹⁾The article was presented at 5th Polish Congress of Mechanics & 25th International Conference on Computer Methods in Mechanics, September 7, 2023, Gliwice.

ensuring it constitutes the optimal solution in subsequent phases. This imperative is particularly pronounced in large-scale projects, where arbitrary geometry parameters at the conceptual stage could result in significant additional material costs.

The aforementioned engineering challenge can be framed as a multi-parametric and multi-criteria optimization problem. Even for a single structure, multiple geometric decision variables can be identified, including cross-section parameters, height, width, or the number of elements. Various structural criteria, such as bearing capacity or admissible deflection, can also be formulated. Consequently, the global optimization problem may involve a multitude of parameters and criteria. Managing a large number of global parameters and optimization criteria can lead to a complex and resource-intensive problem. However, the availability of effective numerical algorithms for global multi-parametric multi-criteria optimization is limited. Additionally, ensuring control over the optimal solution for each specific structural element can be challenging within the context of global optimization. Considering these aspects, there is a compelling need to develop a flexible approach aimed at providing structural topological optimization for complex structural systems at all stages of design.

1.2. State-of-the-art

In the realm of structural optimization, contemporary scientific research has yielded numerous approaches, as outlined by Rozvany [1, 2]. A classification proposed by Rozvany includes Layout Optimization (LO), Generalized Shape Optimization (GSO), and a combined approach (LO + GSO) for composite structures. LO involves the analysis of grid-like bar structures with parallel optimization, while GSO is primarily associated with plain stress problems. SIGMUND [3] provided a comprehensive review of various optimization approaches.

Generalized shape optimization is commonly considered, employing diverse methods such as the co-rotational method [4], subdivision and simplification [5], adjoined methods with non-linearity [6], reduced-order modeling [7], extended multi-scale finite element methods with hierarchy [8], and local and global buckling analyses [9]. Additionally, reliability estimation methods are incorporated [10–12]. Bayesian optimization [13] has been proposed as a non-gradient approach with a probabilistic model.

While generalized shape optimization methods find applications in various engineering fields, they are less effective for structural systems in buildings due to the different designing approach. Building structures are typically designed by analyzing individual members rather than treating the structure as a material continuum.

For the optimization of bar structures, a multi-dimensional and single-objective optimization problem arises with constraints and decision variables of mixed numerical types (Boolean, integer, real). Various approaches have been formulated, relying on stochastic methods (genetic algorithms [14] or other biologically inspired algorithms [15]) and deterministic solutions. Deterministic approaches include non-gradient methods such as joint penalty and material selection [16], gradient-free proportional optimization [17], and buckling constraints for spatial trusses [18]. Gradient methods, such as non-smooth steepest descent algorithms [19], have also been explored.

Less conventional techniques have been reported, such as the application of the so-called political optimizer [20], optimization with discrete variables [21, 22], and Eurocode-compliant optimization [23]. Multi-objective optimization problems may be addressed using simplified or full approaches, with criteria considered separately (e.g., bars exchange method [24] for topology and geometry optimization) or in an averaged manner [25]. The construction of a Pareto front is an alternative, albeit computationally demanding [26, 27].

While these approaches effectively tackle individual problems with global parameters, they often lack the granularity needed to achieve sufficient control over the optimal solution for each specific element in structural systems of buildings. A generalized approach applicable to various structural systems is essential for buildings design. Otherwise, formulating a global optimization problem for the entire structure may be time-consuming and less effective.

Commercial software based on parametric design includes Grasshopper 3D, CATIA, Dynamo, SolveSpace, and ParaCloud. Optimization packages are offered by software such as Altair (OptiStruct, SolidThinking Inspire), Ansys (Mechanical Topology Optimization), Autodesk (Inventor Shape Generator, Within), Dassault (Solidworks Simulation Topology Optimization), Siemens (Optistruct using VTS), and Dlubal RFEM. These packages, however, predominantly rely on GSO.

1.3. Proposed solution approach

We propose a solution approach that embraces the innovative concept of structural patterns. This concept rests on the premise that the structure can be decomposed into several typical patterns (sets of elements) with a reduced number of decision variables. Consequently, a set of smaller optimization problems is addressed reliably, replacing the analysis performed at the global level. Subsequently, selected design parameters corresponding to these patterns undergo numerical optimization. Each pattern may necessitate its optimization algorithm, deterministic or stochastic, chosen based on factors such as expected solution accuracy, computational time, the ability to calculate the gradient of the objective function, and the number of objective function values.

The type of algorithm and its control parameters are determined through a series of benchmark tests. Particularly for the most promising gradient deterministic approaches, such as conjugate gradients and the Newton method, we introduce several novel ideas to enhance their operational quality. Firstly, finite difference schemes are applied to compute the gradient and Hessian of the objective function, with values obtained from a simple finite element model for bar structures. Additionally, a step size corresponding to the search direction is evaluated at each iteration step using a simple iterative method based on the dichotomous division of the search interval. This approach mitigates the serious drawbacks of gradient methods with the highest convergence rates, such as the Newton method, eliminating the risk of solution divergence and sensitivity to the selection of an initial guess solution. Consequently, selected deterministic methods can be competitive with time-consuming and computationally demanding stochastic approaches. This allows for the effective analysis of problems requiring the determination of a family of optimal solutions, either separately or through parallel techniques, such as the determination of convergence maps (for benchmark tests) or reliability analysis (for real engineering problems). Ultimately, the interaction between patterns is managed with control over each optimized pattern during computations. All results presented for executed examples were obtained using our proprietary software, developed primarily in MATLAB and complemented by selected toolboxes dedicated to finite element modeling and genetic algorithms.

The paper is organized as follows: Sec. 2 presents the general formulation of the multidimensional and multi-objective optimization problem. In Sec. 3, we outline the general principles of applied computational approaches, with a particular focus on the novel elements introduced into the optimization algorithms of deterministic types. The paper is enriched with results from typical benchmark tests and selected engineering optimization problems (Sec. 4) for structures described parametrically, including bending beams, vertical trusses, and combinations of truss and beam patterns. Load schemes with both fixed and uncertain parameters (location, magnitude) are taken into account. The paper concludes briefly, highlighting directions for future work.

2. PROBLEM FORMULATION

The vector of decision variables (design parameters)

$$(2.1) \quad \mathbf{d} = [\mathbf{b} \quad \mathbf{z} \quad \mathbf{r}]$$

may contain subvectors consisting of variables of various numerical types, including:

- $\mathbf{b} = [b_1 \ b_2 \ \dots \ b_{n_b}] \in \{ 0 \ 1 \}^{n_b}$ – vector of Boolean variables (e.g., existence or non-existence of selected bars or supports),
- $\mathbf{z} = [z_1 \ z_2 \ \dots \ z_{n_z}] \in \mathbb{Z}^{n_z}$ – vector of integer variables (e.g., number of bars, hinges or supports),
- $\mathbf{r} = [r_1 \ r_2 \ \dots \ r_{n_r}] \in \mathbb{R}^{n_r}$ – vector of rational/real variables (e.g., bar length, span, cross-section dimensions).

The total number of decision variables is denoted as $n_d = n_b + n_z + n_r$. Afterwards, a multidimensional and multi-valued objective function may be formulated as:

$$(2.2) \quad \mathbf{F}(\mathbf{d}) = [F_1(\mathbf{d}) \ F_2(\mathbf{d}) \ \dots \ F_{n_f}(\mathbf{d})] \in \mathbb{R}^{n_f}.$$

Its components correspond to appropriate optimization criteria. Among them one may distinguish the following ones, namely

- maximum displacement/deflection $F_i(\mathbf{d}) = \max_{(\xi)} |v(\mathbf{d}, \xi)|$,
- capacity (e.g., maximum bending moment) $F_i(\mathbf{d}) = \max_{(\xi)} |M(\mathbf{d}, \xi)|$,
- selected/average reaction force $F_i(\mathbf{d}) = |R(\mathbf{d})|$,
- critical force $F_i(\mathbf{d}) = P_{\text{crit}}^{-1}(\mathbf{d})$,
- frequency of eigen vibrations $F_i(\mathbf{d}) = \omega^{-1}(\mathbf{d})$,
- total volume of bars $F_i(\mathbf{d}) = A(\mathbf{d}) \rho$,
- minimum number of plastic hinges,

and others. In the given examples, F_i denotes a selected component of the vector objective function $\mathbf{F}(\mathbf{d})$ as defined in Eq. (2.2). Here, i ranges from 1 to n_f , where n_f represents the number of objective functions, and $\xi \in \mathbb{R}$ represents the scalar physical coordinate corresponding to the local coordinate system attached to a particular bar. In the general case, determining both the maximum displacement and bending moment (among other generalized cross-sectional forces) requires solving an additional local optimization problem for a single decision variable ξ with a fixed vector of decision variables \mathbf{d} . Simplified approaches may involve examining their values at specified points of a structure, such as midpoints of spans, hinges, and supports. In addition to local criteria, which are adopted in this research, global criteria may also be considered [28]. For instance, global functional of potential (or complementary) energy can be defined as the work of external forces on the displacements caused by subjected loads instead of local minimization problems mentioned above. Although the final optimal solution is obtained in the global sense and therefore may be different from the one obtained by means of local criteria, the solution of additional optimization problem may be omitted for each \mathbf{d} in favor of the integration procedure performed on the entire structure. However, such an approach is not considered in this research.

Typically, the vector \mathbf{d} is determined within the admissible domain Ω_{adm} . In cases where no other constraints are formulated, Ω_{adm} is defined by admissible intervals for each component of the decision variable vector, namely:

$$(2.3) \quad \Omega_{\text{adm}} = \left\{ \left(b_i \in \{0 \ 1\} \quad z_j \in \left[z_j^{\min} \quad z_j^{\max} \right] \quad r_k \in \left[r_k^{\min} \quad r_k^{\max} \right] \right) \right\},$$

where

$$(2.4) \quad i = 1, 2, \dots, n_b, \quad j = 1, 2, \dots, n_z, \quad k = 1, 2, \dots, n_r.$$

Furthermore, additional n_{eq} equality and n_{ineq} inequality constraints may be formulated as well, thus reshaping Ω_{adm} , for instance related to the geometric constraints of the optimized structure:

$$(2.5) \quad \mathbf{R}_{\text{eq}}(\mathbf{d}) = \mathbf{0}, \quad \mathbf{R}_{\text{ineq}}(\mathbf{d}) < \mathbf{0},$$

where R_{eq} and R_{ineq} are $n_{\text{eq}} \times 1$ and $n_{\text{ineq}} \times 1$ vectors, respectively. In the case where the parametric description is applied to structure modeling, the conditions R_{eq} and R_{ineq} relate relevant components of the decision vector \mathbf{d} through explicit algebraic relations of linear or quadratic forms. These conditions originate from design limitations (e.g., the total volume of steel or total bar length) and are therefore fully differentiable and convex (in the linear case) with respect to the optimization conditions. These constraints do not stem from functional restrictions; thus, global and local limitations (e.g., stability or plastic condition) must be assessed through the components of the objective function itself. Moreover, equality conditions of considered type may be introduced to the objective function using simple elimination methods (for the linear case) or Lagrange multipliers (for the quadratic case). On the other hand, inequality conditions may require special treatment, such as the application of the feasible direction method. However, such conditions are not considered in the current research.

2.1. Single-objective optimization

In the simplest case, one deals with only one optimization criterion, hence the multidimensional objective function is the function of one real decision variable at least ($n_d \geq n_r \geq 1$), whereas it constitutes a single-valued function ($n_f = 1$). Therefore, the optimization problem may be considered as the determination of the minimum of the objective function (2.2) with respect to the vector of decision variables:

$$(2.6) \quad \min_{(\mathbf{d})} F(\mathbf{d}) \quad \text{for} \quad \mathbf{d} \in \Omega_{\text{adm}}.$$

Consequently, its optimal solution may be defined as follows:

$$(2.7) \quad \mathbf{d}^{(\text{opt})} = \arg \min_{\mathbf{d}} F(\mathbf{d}) \quad \text{for} \quad \mathbf{d}^{(\text{opt})} \in \Omega_{\text{adm}}.$$

In order to guarantee the existence of the optimal solution, the appropriate Kuhn-Tucker conditions [29] must be satisfied. In the case of a non-constrained optimization problem, these conditions have a simplified form and can be separated into necessary

$$(2.8) \quad \nabla_{\mathbf{d}} F(\mathbf{d}) = \mathbf{0}, \quad \nabla_{\mathbf{d}} F(\mathbf{d}) = \left\{ \frac{\partial F}{\partial d_l}, \quad l = 1, 2, \dots, n_d \right\}$$

and sufficient conditions

$$(2.9) \quad \mathbf{y}^T \mathbf{H}(\mathbf{d}) \mathbf{y} > 0, \quad \forall \mathbf{y} \in \mathbb{R}^{n_d} \neq \mathbf{0},$$

where

$$(2.10) \quad \mathbf{H}(\mathbf{d}) = \nabla_{\mathbf{d}} \otimes \nabla_{\mathbf{d}} F(\mathbf{d}).$$

Therefore, the gradient (vector of first-order derivatives of the objective function) and Hessian (matrix of second-order derivatives of the objective function) have to be computed. It may be noticed that the positive definiteness of the Hessian (2.9) provides the convexity of the objective function, required for most of the deterministic methods, discussed in the following section.

2.2. Multi-objective optimization

In the general case, when dealing with multi-criteria optimization ($n_f > 1$), the criteria mentioned above, which are valid for $n_f = 1$, cannot be directly extended and reformulated. In such scenarios, it is infeasible to identify a solution where all objective functions attain their minimum values simultaneously. This challenge arises because the objective functions represent criteria that are inherently incompatible with each other. In other words, minimizing one function might lead to an increase in the others. In such cases, we characterize the dominance of one criterion over the others, which can be expressed symbolically as follows:

$$(2.11) \quad \mathbf{d}_j \succ \mathbf{d}_k \iff \exists_{l \in [1 \dots n_f]} F_l(\mathbf{d}_j) \leq F_l(\mathbf{d}_k),$$

namely the solution \mathbf{d}_j dominates over the solution \mathbf{d}_k if and only if $F_l(\mathbf{d}_j)$ is not greater than $F_l(\mathbf{d}_k)$. Hence, a division of potential solutions from the space of feasible solutions (i.e., those for which the vector objective function

yields finite values) into dominated and non-dominated solutions is introduced. A solution is considered non-dominated when it is not possible to find a superior solution with respect to at least one criterion without compromising others. The non-dominated subset of the entire feasible decision space is termed the Pareto-optimal set. The boundary, defined by the set of all points mapped from the Pareto optimal set, is termed the Pareto optimal front of efficient solutions. The primary objective is to identify a set of diverse solutions as closely positioned to the Pareto-optimal front as possible. Therefore, the selection of a single optimal solution $\mathbf{d}^{(\text{opt})}$ in multi-criteria optimization is ambiguous and typically results from the adoption of additional assumptions in an approximate manner [26, 27, 30, 31].

The simplest, albeit primitive, approach involves solving n_f separate single-objective problems and obtaining a weighted average solution:

$$(2.12) \quad \min_{(\mathbf{d})} F_l(\mathbf{d}) \rightarrow \mathbf{d}_l^{(\text{opt})}, \quad l = 1, 2, \dots, n_f \rightarrow \mathbf{d}^{(\text{opt})} \approx \sum_{l=1}^{n_f} \omega_l \mathbf{d}_l^{(\text{opt})}, \quad \sum_{l=1}^{n_f} \omega_l = 1.$$

It is worth noting that non-negative weights $\omega_l \geq 0$ are entirely optional and can be used to control the influence of specific criteria. Typically, this approach yields dominated Pareto solutions and serves as a starting point for more sophisticated methods. One of its important modifications is the ε -constrained method, in which only one objective function is optimized while the others are constrained within user-specified values and treated as additional inequality constraints:

$$(2.13) \quad \min_{(\mathbf{d})} F_i(\mathbf{d}), \quad F_l(\mathbf{d}) \leq \varepsilon_l \rightarrow \mathbf{d}^{(\text{opt})}, \quad i \in [1 \ n_f], \quad l = 1, 2, \dots, n_f, \quad l \neq i.$$

This approach is applicable to both convex and non-convex problems. However, the selection of ε values requires special care to ensure that they are within the minimum or maximum values of the individual objective functions.

The most commonly applied approach is based on the weighted sum method, wherein a set of objectives is scalarized into a single objective by adding each objective pre-multiplied by user-supplied weights:

$$(2.14) \quad F(\mathbf{d}) = \sum_{l=1}^{n_f} \omega_l F_l(\mathbf{d}) \rightarrow \min_{(\mathbf{d})} F(\mathbf{d}) \rightarrow \mathbf{d}^{(\text{opt})}, \quad \sum_{l=1}^{n_f} \omega_l = 1.$$

Similarly as in Eq. (2.12), the non-negative weight ($\omega_l \geq 0$) of each objective is chosen in proportion to its relative importance. Moreover, it is also used to de-dimensionalize individual components. Although simple, it is challenging to set weights to obtain a Pareto-optimal solution in a desired region of the objective space. Furthermore, this method may fail to find certain Pareto-optimal solutions in non-convex objective spaces.

Eventually, in the weighted metric method, multiple objective functions are combined using the weighted distance metric of any solution from the ideal solution $\mathbf{F}^{(\text{opt})}$, namely:

$$(2.15) \quad \min_{(\mathbf{d})} L_p(\mathbf{d}) \rightarrow \mathbf{d}^{(\text{opt})}, \quad L_p(\mathbf{d}) = \left(\sum_{l=1}^{n_f} \omega_l \left| F_l(\mathbf{d}) - F_l^{(\text{opt})} \right|^p \right)^{1/p}.$$

For simple cases ($p = 1$ and $p = 2$), this method yields the same solution as the weighted sum method. Moreover, the weighted Tchebycheff metric (for $p = \infty$) guarantees the determination of all Pareto-optimal solutions with the ideal solution $\mathbf{F}^{(\text{opt})}$. However, this method requires knowledge of the minimum and maximum objective values as well as $\mathbf{F}^{(\text{opt})}$, which may be found by independently optimizing each objective function as in (2.12). For small p , not all Pareto-optimal solutions are obtained, and as p increases, the problem becomes non-differentiable.

In addition to the aforementioned traditional approaches that require standard computational tools, there are several different multi-objective evolutionary algorithms belonging to the wide group of genetic algorithms, which are briefly discussed in the following chapter.

3. COMPUTATIONAL APPROACHES

The effective analysis of the optimization problem using analytical methods is possible only for the simplest cases. This limitation arises because the analytical form of the objective function is unknown, making it feasible to calculate values point-wise only. Consequently, both the objective function values and its derivatives need to be computed numerically, assuming differentiability. As a result, appropriate numerical frameworks are necessary at both the optimization and construction levels of analysis. The determination of the deformation state for the fixed set of variables \mathbf{d} , transferred from the optimization level, is based on the standard finite element method (FEM) in the displacement formulation.

3.1. Finite element model

Selected bar problems are analyzed in the first stage of the research, employing linear elasticity theory, namely Hooke’s law, small deformations, and Euler-Bernoulli assumptions. Standard truss and enhanced beam finite elements are illustrated in Fig. 1a and Fig. 1b, respectively.

For the 2D truss element with two degrees of freedom q_1, q_2 , two linear Lagrange shape functions $L_1^{(1)}, L_2^{(1)}$ are applied to interpolate the displacement

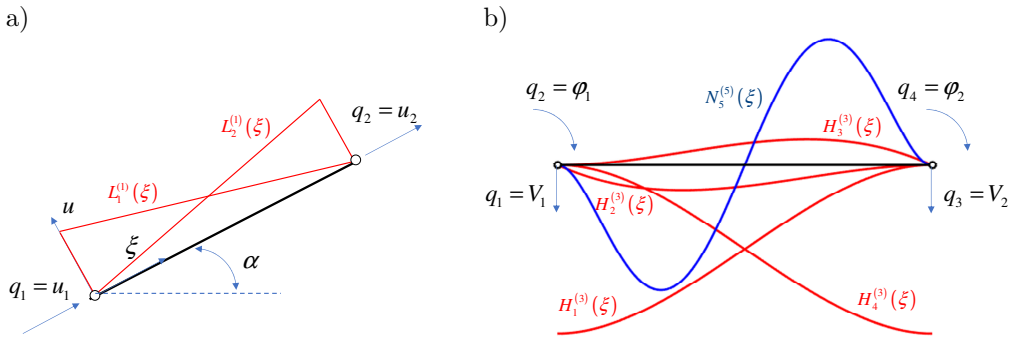


FIG. 1. Finite elements applied for bar structures:
 a) 2D truss element, b) enhanced beam element.

function u at the local coordinate system (ξ, u) . In the case of the beam element with four degrees of freedom q_1, q_2, q_3, q_4 , standard Hermite interpolation of the deflection field is used

$$(3.1) \quad v(\xi) = \overbrace{\sum_{i=1}^4 q_i H_i^{(3)}(\xi)}^{\text{SAE generation + post-processing}} + \overbrace{N_5^{(5)}(\xi)}^{\text{post-processing}},$$

with cubic shape functions $H_1^{(3)}, H_2^{(3)}, H_3^{(3)}, H_4^{(3)}$. Moreover, the interpolation formula (3.1) is a-posteriori enhanced by means of the additional component with the fifth-order polynomial function $N_5^{(5)}$ that corresponds to the particular integral of the Bernoulli beam deflection equation for trapezoidal load. This enhancement allows for the reproduction of the polynomial solution up to and including the fifth order at every point of the considered structure. Therefore, both discretization and approximation errors are zero (up to machine precision) for static problems, regardless of the mesh density. On the other hand, the accuracy of the solution for dynamic and buckling problems strongly depends on the number of finite elements applied for each bar.

Computation of the local quantities at the element level is followed by their transformation and aggregation into the global system of simultaneous algebraic equations (SAE). These may include the stiffness matrix \mathbf{K} as well as the load vector \mathbf{P} (for static and buckling problems), consistent mass matrix \mathbf{M} (for dynamic problems), as well as the matrix of initial stresses \mathbf{K}_σ (for buckling problems). In the simplest cases, the solution of SAE with global matrices and vectors, accounting for boundary conditions (with the lower index bc), explicitly yields the specified l -th component F_l of the objective function \mathbf{F} , depending on the problem type, namely:

– static problem

$$\begin{aligned}
 \mathbf{K}(\mathbf{d}) \mathbf{Q} = \mathbf{P}(\mathbf{d}) \rightarrow & \begin{cases} \mathbf{Q}(\mathbf{d}) = \mathbf{K}_{bc}^{-1}(\mathbf{d}) \mathbf{P}_{bc}(\mathbf{d}) \\ \mathbf{R}(\mathbf{d}) = \mathbf{K}(\mathbf{d}) \mathbf{Q}(\mathbf{d}) - \mathbf{P}(\mathbf{d}) \end{cases} \rightarrow \\
 (3.2) \quad & \rightarrow \mathbf{s}^e(\mathbf{d}) \rightarrow F_l(\mathbf{d}) = \begin{cases} \max \mathbf{Q}(\mathbf{d}) \\ \max \mathbf{R}(\mathbf{d}) \\ \max \mathbf{s}^e(\mathbf{d}) \\ \dots \end{cases},
 \end{aligned}$$

– eigen dynamic problem

$$(3.3) \quad (\mathbf{K}(\mathbf{d}) - \omega^2 \mathbf{M}(\mathbf{d})) \mathbf{Q} = \mathbf{0} \rightarrow F_l(\mathbf{d}) = \frac{1}{\omega_{\min}(\mathbf{d})},$$

– buckling problem with \mathbf{K}_σ computed from statics

$$(3.4) \quad (\mathbf{K}(\mathbf{d}) + \lambda \mathbf{K}_\sigma(\mathbf{d})) \mathbf{Q} = \mathbf{0} \rightarrow F_l(\mathbf{d}) = \frac{1}{\lambda_{\min}(\mathbf{d})},$$

where \mathbf{Q} represents generalized displacements, \mathbf{R} denotes reaction forces, \mathbf{s}^e stands for generalized forces at the element level, ω represents eigenfrequencies, and λ signifies load configuration multipliers.

In more complex scenarios, such as beam bending problems under static load, where the objective is to minimize the maximum values of deflection v_{\max} and/or generalized forces (bending moment M_{\max} and shear force Q_{\max}), an additional local optimization problem arises. In this case, the entire mesh of elements (when searching for global maximal values) or specified elements only (when examination is limited to parts of a structure) must be examined. It is crucial to solve this problem without introducing additional approximation errors. To achieve this, local interpolation (3.1) is applied and differentiated to satisfy the necessary conditions for the existence of the optimum for each specified quantity, namely

$$(3.5) \quad v_{\max} \rightarrow \frac{dv}{d\xi} = 0, \quad M_{\max} \rightarrow \frac{d^3v}{d\xi^3} = 0, \quad Q_{\max} \rightarrow \frac{d^4v}{d\xi^4} = 0, \quad \xi \in [0 \quad l^e].$$

Therefore, the local optimization problem involves determining the roots of relevant polynomial equations (of fourth, second, and first orders, respectively) derived from conditions (3.5) within the finite element with length l^e .

Subsequently, the objective function values $\mathbf{F}(\mathbf{d})$ are transferred back to the optimization level.

3.2. Finite difference schemes

Even for the simplest unconstrained single-objective optimization problems, it may be necessary to evaluate both the gradient (2.8) for determining the existence of the minimum and the Hessian (2.10) for examining the convexity of the scalar objective function F with respect to the vector of decision variables \mathbf{d} . Moreover, assuming that \mathbf{d} consists of real variables only ($n_d = n_r$), algorithms of deterministic methods of gradient type effectively utilize the gradient (or gradient and Hessian) at all iteration steps. In the general case, computing derivatives of the objective function F can be challenging, especially when, for a fixed \mathbf{d} , solving the additional local optimization problem (3.5) for a scalar decision variable ξ is required. If the analytical formula of F with respect to both \mathbf{d} and ξ is unknown or difficult to obtain, its values can only be evaluated point-wise for a fixed vector \mathbf{d} of decision variables. For linear static problems, the gradient and the Hessian of the objective function require direct differentiation of the nodal FE solution obtained from Eq. (3.2). For instance, the gradient of the general displacement vector \mathbf{Q} may be computed as follows:

$$(3.6) \quad \frac{\partial \mathbf{Q}}{\partial \mathbf{d}} = \frac{\partial \mathbf{K}_{bc}^{-1}}{\partial \mathbf{d}} \mathbf{P}_{bc}(\mathbf{d}) + \mathbf{K}_{bc}^{-1}(\mathbf{d}) \frac{\partial \mathbf{P}_{bc}}{\partial \mathbf{d}},$$

the equation commonly appears in sensitivity analysis [32–34]. Although both derivatives in Eq. (3.6) can be computed directly and analytically (e.g., in linear bar models), this process can be computationally demanding (e.g., in the case of nonlinear theory) and challenging to automate for both the objective function and the analyzed problem of arbitrary types, particularly when FE toolboxes are used in a black-box style. Therefore, an appropriate numerical approach may be carried out instead of the direct application of formula (3.6). In contrast to other commonly applied optimization methods in which either the gradient or the Hessian of F is estimated at the optimization level based on two consecutive solutions for \mathbf{d} (quasi-gradient and quasi-Newton methods [35]), we propose the computation of derivatives of F using central finite difference (FD) schemes [36], namely:

$$(3.7) \quad \nabla_{\mathbf{d}} F \approx \frac{F(\mathbf{d} + \Delta \mathbf{d}) - F(\mathbf{d} - \Delta \mathbf{d})}{2\Delta \mathbf{d}} = \begin{bmatrix} \frac{F(d_1 + \Delta d_1) - F(d_1 - \Delta d_1)}{2\Delta d_1} \\ \frac{F(d_2 + \Delta d_2) - F(d_2 - \Delta d_2)}{2\Delta d_2} \\ \dots \\ \frac{F(d_{n_d} + \Delta d_{n_d}) - F(d_{n_d} - \Delta d_{n_d})}{2\Delta d_{n_d}} \end{bmatrix}$$

and

$$(3.8) \quad \mathbf{H}(\mathbf{d}) = \nabla_{\mathbf{d}} \nabla_{\mathbf{d}}^T F \approx \frac{\nabla_{\mathbf{d}} F(\mathbf{d} + \Delta \mathbf{d}) - \nabla_{\mathbf{d}} F(\mathbf{d} - \Delta \mathbf{d})}{2\Delta \mathbf{d}},$$

where $\Delta \mathbf{d}$ is the vector of solution increments, relatively small with respect to admissible limits (Eq. (2.3)) for \mathbf{d} . However, to avoid numerical instability, these increments should not be smaller than 10^{-6} . In this manner, the computation of (3.7) requires $2n_d$ objective function values, whereas one needs $\frac{1}{2}n_d(n_d + 1)$ values for the computation of (3.8). Since the same values appear in both FD formulas, the total number of required objective function values should not exceed n_d^2 . The accuracy of these formulas is relatively high and could be estimated as $O(h^2)$.

It is important to emphasize that this approach is anticipated to work effectively when dealing with decision variables of real type exclusively. For decision variables of integer and/or Boolean types, non-gradient optimization approaches must be employed.

3.3. Deterministic methods

Back at the global level, the simplest deterministic methods construct the chain of approximated solutions starting from the initial guess solution \mathbf{d}^0 to the final optimal solution \mathbf{d}^{opt} , namely:

$$(3.9) \quad \mathbf{d}^{k+1} = \mathbf{d}^k + \alpha^k \mathbf{h}^k, \quad k = 0, 1, 2, \dots,$$

where \mathbf{d}^k and \mathbf{d}^{k+1} denote two subsequent solution approximations, k is the iteration number, α^k is the step size, and \mathbf{h}^k denotes the search direction. A variety of deterministic methods exist, differing in the manner the search direction is calculated at each iteration step (global level). In the case of non-gradient methods, the n_d trial searches have to be performed separately with an additional one being the conjugated direction (Powell method, Nelder-Mead simplex method). The steepest descent and conjugate gradients methods require computation of the objective function gradient $\nabla_{\mathbf{d}} F(\mathbf{d}^k)$, whereas the Newton method additionally uses information concerning its Hessian $\nabla_{\mathbf{d}} \nabla_{\mathbf{d}}^T F(\mathbf{d}^k)$.

The solution convergence rate p of deterministic methods, defined as follows:

$$(3.10) \quad \frac{\|\mathbf{d}^{k+1} - \mathbf{d}^{\text{opt}}\|}{\|\mathbf{d}^k - \mathbf{d}^{\text{opt}}\|^p} \leq C, \quad C \in (0 \ 1),$$

is rather small and varies from 1 to 2. Moreover, final solutions are very sensitive to the selection of \mathbf{d}^0 . However, the key issue is the appropriate selection of the step size α^k (with the exception of the simplex method). Generally, it should be

determined as the optimal solution of the auxiliary one-dimensional directional optimization problem (local level), namely

$$(3.11) \quad \alpha^k = \arg \min_{\alpha} f(\alpha), \quad f(\alpha) = F(\mathbf{d}^k + \alpha \mathbf{h}^k).$$

As this problem cannot be solved directly, two main approaches have been reported in the literature [35, 37]. One possibility is to apply line search in which the optimal α^k is determined by a relevant sampling technique (starting from $\alpha = 0$ and moving forwards) and observing values of f . The second one assumes the approximation of α^k by means of closed-form formulas, composed of solutions for \mathbf{d} from previous iteration steps at the global level. However, both approaches do not guarantee the determination of the globally optimal solution of Eq. (3.11). Moreover, the wrong selection of α^k may cause a solution divergence (or convergence to a solution located outside the admissible domain). Therefore, our proposal is based on the reliable selection of enclosing bounds for α as well as the well-known bisection method in two alternative variants. Consequently, solution divergence for both \mathbf{d} and α may be avoided in favor of slower convergence.

Firstly, interval bounds are selected by substituting the admissible domain limits Eq. (2.3) into Eq. (3.9) and evaluating relevant norms, namely:

$$(3.12) \quad \alpha_{\text{left}} = \varepsilon > 0, \quad \alpha_{\text{right}} = s \min \left[\frac{\|\mathbf{d}^{\min} - \mathbf{d}^k\|}{\|\mathbf{h}^k\|}, \frac{\|\mathbf{d}^{\max} - \mathbf{d}^k\|}{\|\mathbf{h}^k\|} \right],$$

where the scalar parameter s has to be selected in an iterative manner. In most cases, one may start with $s = 1$ and perform subsequent decreases until the admissible location of \mathbf{d} is reached. Afterwards, the interval $[\alpha_{\text{left}} \ \alpha_{\text{right}}]$ is divided into two equal parts by determining the middle point:

$$(3.13) \quad \alpha_{\text{middle}} = \frac{1}{2} (\alpha_{\text{left}} + \alpha_{\text{right}}).$$

Two variants are possible: non-gradient and gradient bisection methods. In the case of the simpler, though more primitive, non-gradient bisection, one has:

$$(3.14) \quad C = f(\alpha_{\text{left}}) < f(\alpha_{\text{right}}).$$

Gradient bisection may be implemented as follows:

$$(3.15) \quad \begin{aligned} \nabla_{\text{left}} f &= \mathbf{h}^k \frac{df}{d\alpha}(\alpha_{\text{left}}) = \frac{\mathbf{h}^k}{2\Delta\alpha} (f(\alpha_{\text{left}} + \Delta\alpha) - f(\alpha_{\text{left}} - \Delta\alpha)), \\ \nabla_{\text{middle}} f &= \mathbf{h}^k \frac{df}{d\alpha}(\alpha_{\text{middle}}) = \frac{\mathbf{h}^k}{2\Delta\alpha} (f(\alpha_{\text{middle}} + \Delta\alpha) - f(\alpha_{\text{middle}} - \Delta\alpha)), \end{aligned}$$

$$C = \nabla_{\text{left}} f \nabla_{\text{middle}}^T f < 0,$$

where a similar concept using central finite difference operators is incorporated, as in the case of (3.7). A small yet finite increment $\Delta\alpha > 10^{-6}$ may be selected based on the admissible interval for α . Furthermore, in the case where the scalar parameter $C = 1$, $\alpha_{\text{right}} = \alpha_{\text{middle}}$, or $\alpha_{\text{left}} = \alpha_{\text{middle}}$. For each internal iteration step, the number of required values of the objective function is equal to 1 (non-gradient variant) or 2 (gradient variant). The only exception is the first step, where these numbers should be doubled.

Break-off tests may include examination of the following indicators:

$$(3.16) \quad \frac{\|\mathbf{d}^{k+1} - \mathbf{d}^k\|}{\|\mathbf{d}^{k+1}\|} < \varepsilon_d, \quad \frac{\|F(\mathbf{d}^{k+1}) - F(\mathbf{d}^k)\|}{\|F(\mathbf{d}^0)\|} < \varepsilon_f, \quad \frac{\|\nabla_{\mathbf{d}}F(\mathbf{d}^{k+1})\|}{\|\nabla_{\mathbf{d}}F(\mathbf{d}^0)\|} < \varepsilon_g,$$

namely, convergence rate, quality index and gradient residuum (for gradient methods), respectively. In above formulas ε_d , ε_f , ε_g denote assumed admissible errors. Moreover, the number of iterations $k < k_{\text{max}}$ should be controlled as well. Algorithm efficiency may be defined as the number of required evaluations of objective function values (N_f). The general flow chart of methods of deterministic type applied to unconstrained optimization problem, assuming the admissible domain Ω_{adm} as defined in Eq. (2.3), is presented in Fig. 2 with novel elements highlighted using blocks with bold red edges. In case the equality and/or inequality constraints (Eq. (2.5)) are present, all developed algorithms remain applicable, though they must be extended to incorporate modifications ensuring that the search direction is not only effective in minimizing the objective function but feasible as well. For instance, the simplex approach may be employed for this purpose.

3.4. Genetic algorithms

Deterministic optimization approaches may effectively work with decision variables of real type only ($n_d = n_r$). In case $n_b > 0$ (Boolean type) or $n_z > 0$ (integer type) a modified approach has to be applied. On the other hand, every deterministic method yields the same solution for the same set of input parameters, with accuracy to the equipment used and computational precision. A different concept is presented by genetic algorithms that belong to the group of biologically inspired optimization methods (along with evolutionary algorithms and artificial neural networks [38, 39]). They resemble the functioning of the human immune system in which strong genes (individuals with a low objective function value) are strengthened and weak genes (with a high objective function value) are eliminated. Therefore an entire family of solutions undergoes strongly random processes. Unlike in the case of deterministic methods, every single genetic operation may lead to slightly different results.

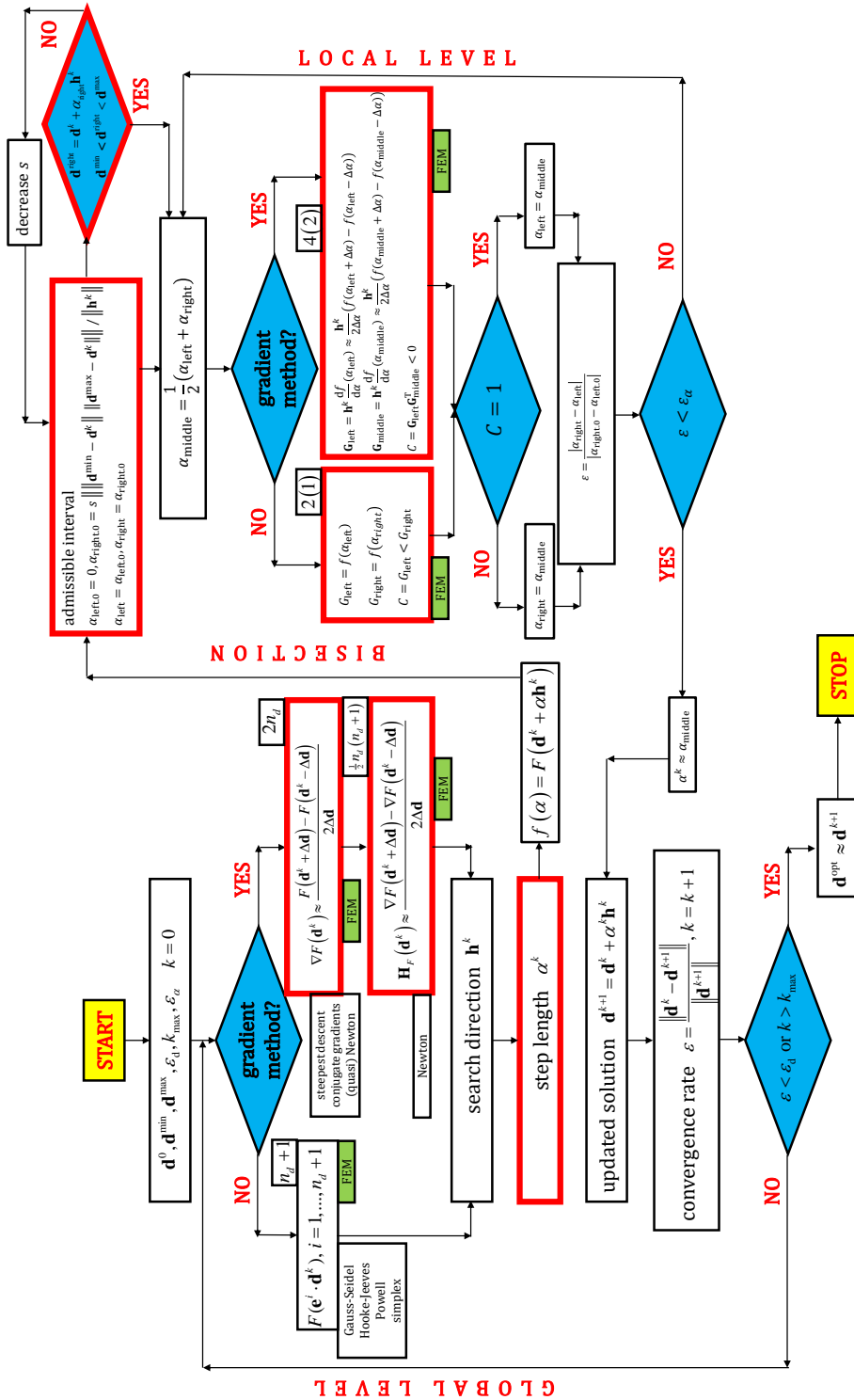


FIG. 2. Deterministic methods – general flow chart.

Each component of decision variables vector \mathbf{d} is coded as a chain of m_b bits whose number corresponds to the required numerical precision. One genetic population consists of m members each of which is a vector composed of n_d binary components. The initial population may be selected randomly or may correspond to the solution obtained from another approach. Nevertheless, population members are frequently modified by means of standard genetic operators, namely selection of roulette type (the only operator that requires values of the objective function), crossover (with probability p_c) and mutation (with probability p_m). In case the equality and/or inequality constraints (2.5) are present, both crossover and mutation operations would need to be adjusted to ensure that each newly generated solution is within the admissible domain before being included in the current population. In most cases, the maximum number of generations m_g is assumed, whereas the brake-off test may involve the admissible participation ε_a of members minimizing the objective function (with accuracy ε_f). The best member (with respect to the objective function value) found throughout all genetic generations is considered as the stochastic estimation of the optimal solution. Alternatively, it may be treated as an entry to the deterministic approach (as the initial solution). The general flow chart of genetic algorithms, taking into account their combinations with FEM and deterministic approaches, is presented in Fig. 3.

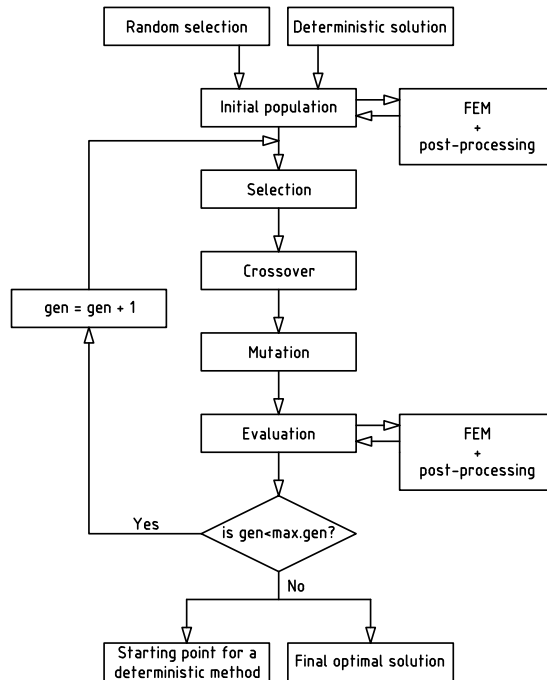


FIG. 3. Genetic algorithms – general flow chart.

3.5. Implementation of patterns

The proposed approach is rooted in the idea of dividing a selected building structure into characteristic patterns, which consist of sets of elements. The study considers several types of patterns that allow for interaction, including horizontal trusses, vertical trusses, and beam grids. These patterns are utilized to compose the structure subjected to optimization. Leveraging the FEM, various optimization techniques, and additional algorithms for interaction, the methodology decomposes the structure into distinct patterns.

Central to this approach is the preliminary sequential algorithm (Fig. 4), which facilitates the optimization of each pattern individually and the transfer of information to subsequent patterns. This information encompasses the loads and geometry of the structure, such as the coordinates of nodes. Additionally, the algorithm aggregates objective function values from each pattern after optimization, which are subsequently employed in global objective functions. Computational examples illustrating this concept are presented in the following section.

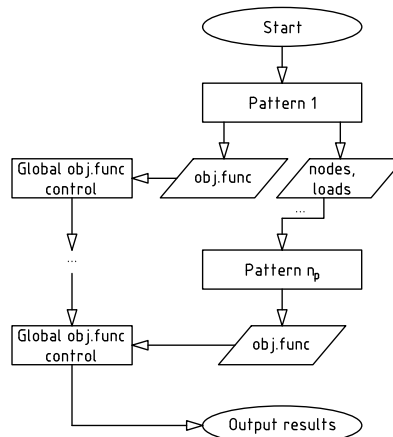


FIG. 4. General flowchart of sequential optimization for the pattern concept.

4. NUMERICAL EXAMPLES

Variety of benchmark tests with known analytical optimal solution, as well as simple engineering problems of statics, dynamics and linearized stability, have been executed. Each time, a combination of FEM with selected optimization methods was considered incorporating a few novel aspects introduced in this paper. Special emphasis has been laid upon the combination of FEM with FD schemes. Numerical experiments were conducted to assess solution accuracy, the effectiveness of the method (number of objective function values) required,

computational time, as well as algorithm simplicity. The representative results are presented in this section, starting from the simplest tests that could be solved analytically and ending with engineering problems with uncertain load parameters.

4.1. Preliminary results of single-objective optimization

The modified algorithms of selected deterministic methods are preliminarily examined using the benchmark test with the objective function given by the analytical formula. Among the many possible functions, the Rosenbrock function:

$$(4.1) \quad F(\mathbf{d}) = 100(d_2 - d_1^2)^2 + (1 - d_1)^2$$

is chosen for this evaluation [40]. This function, commonly used in optimization problems, presents challenges due to its narrow, curved valley. The goal is to assess the performance and effectiveness of the modified algorithms in handling this particular benchmark test. The admissible interval is assumed as $\mathbf{d} \in [-2 \ 2] \times [-1 \ 3]$. A single minimum of F exists, namely at $\mathbf{d}^{\text{opt}} = [1 \ 1]$, where $F = 0$. For the sake of comparison, the reference solution is determined by the brute search method with a grid of 101×101 middle points.

Afterwards, five different approaches are examined, namely: the Powell conjugate directions method, steepest descent method, conjugate gradient method, Newton method as well as genetic algorithms. First, we perform calculations for one fixed starting point / initial population. For deterministic methods, we assume the initial guess solution as $\mathbf{d}^0 = [-1.5 \ 0]$ with $\varepsilon_d = 10^{-6}$ (only the convergence rate from Eq. (3.16) is examined) and $k_{\text{max}} = 10^3$, $n_d = 2$. For genetic algorithms, the following data is set: $m_b = 20$, $m = 50$, $m_g = 200$, $p_c = 0.7$, $p_m = 0.2$, $\varepsilon_a = 0.2$. The final solutions as well as the averaged convergence rates defined in Eq. (3.10) and obtained for all deterministic approaches are compared in Table 1 for two variants. In the first variant, all derivatives of F and f functions are calculated in an analytical manner, whereas in the second

Table 1. Comparison of solution convergence rates of deterministic approaches with analytical and numerical derivatives of the Rosenbrock function.

Method	Analytical derivatives		Numerical derivatives	
	Final solution	Convergence rate	Final solution	Convergence rate
Powell conjugate directions	[1.111 1.056]	0.472	[1.111 1.056]	0.472
Steepest descent method	[0.896 0.802]	0.878	[0.896 0.802]	0.836
Conjugate gradients method	[1.000 1.000]	0.959	[1.001 1.001]	0.821
Newton method	[1.000 1.000]	2.001	[1.000 1.000]	1.530

one, only FDM schemes (Eqs. (3.7), (3.8) and (3.15)) are applied. Additionally, efficiency of all approaches (brute force search, deterministic methods, genetic algorithms) represented by the number of objective function values computed N_f (blue bars) as well as gradients (red bars) and Hessian matrix (green bar) is compared in Fig. 5.

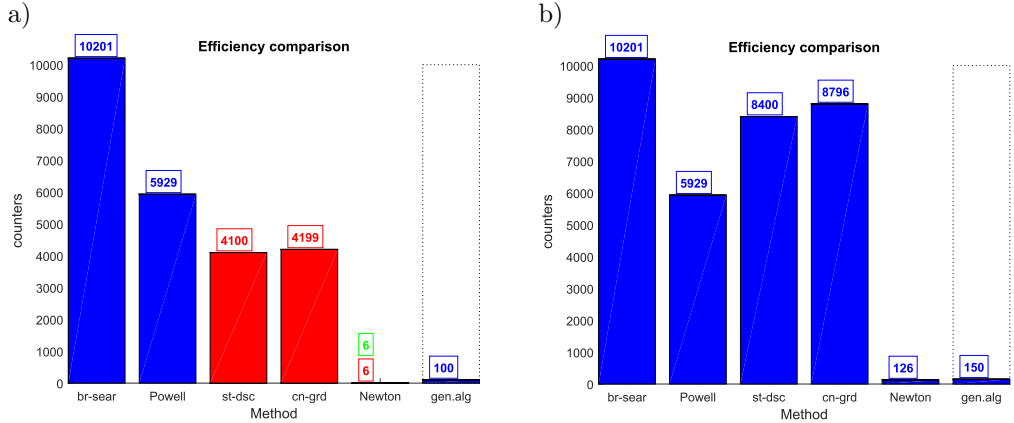


FIG. 5. Comparison of methods' efficiency for the Rosenbrock function and a) analytical derivatives, b) numerical derivatives.

It may be observed that convergence rates of gradient methods are fully comparable when analytical derivatives are replaced by numerical schemes, whereas the number of computed objective function values (Fig. 5b) is similar to the number of gradient components (Fig. 5a). Clearly superior results are obtained for the Newton method with FD schemes, taking both aspects into account. An interesting fact is that N_f for the Newton method (numerical variant) is similar to the one required for genetic algorithms.

Afterwards, more comprehensive tests are performed, namely the generation of convergence graphs for each method. For this purpose, we examine multiple initial guess solutions taken from a regular mesh of 20×20 points (marked as black crosses, see top graphs in Fig. 6a–d and Fig. 7a–c). For each initial solution, the relevant solution algorithm is applied, yielding the approximated optimal solution. In the case of deterministic methods, the relevant iterative process is initialized. In the case of genetic algorithms, the entire initial population consists of the same consecutive solution taken from the solution mesh. A divergent/improper solution is assigned (red field in the bottom maps in Fig. 6e–h and Fig. 7d–f) when the maximum number of iterations is exhausted or the difference between the final solution and the analytical one is greater than 10% (in mean norm). Otherwise, we deal with a convergent process (green field in the above-mentioned maps). The convergence rate is evaluated as the number of

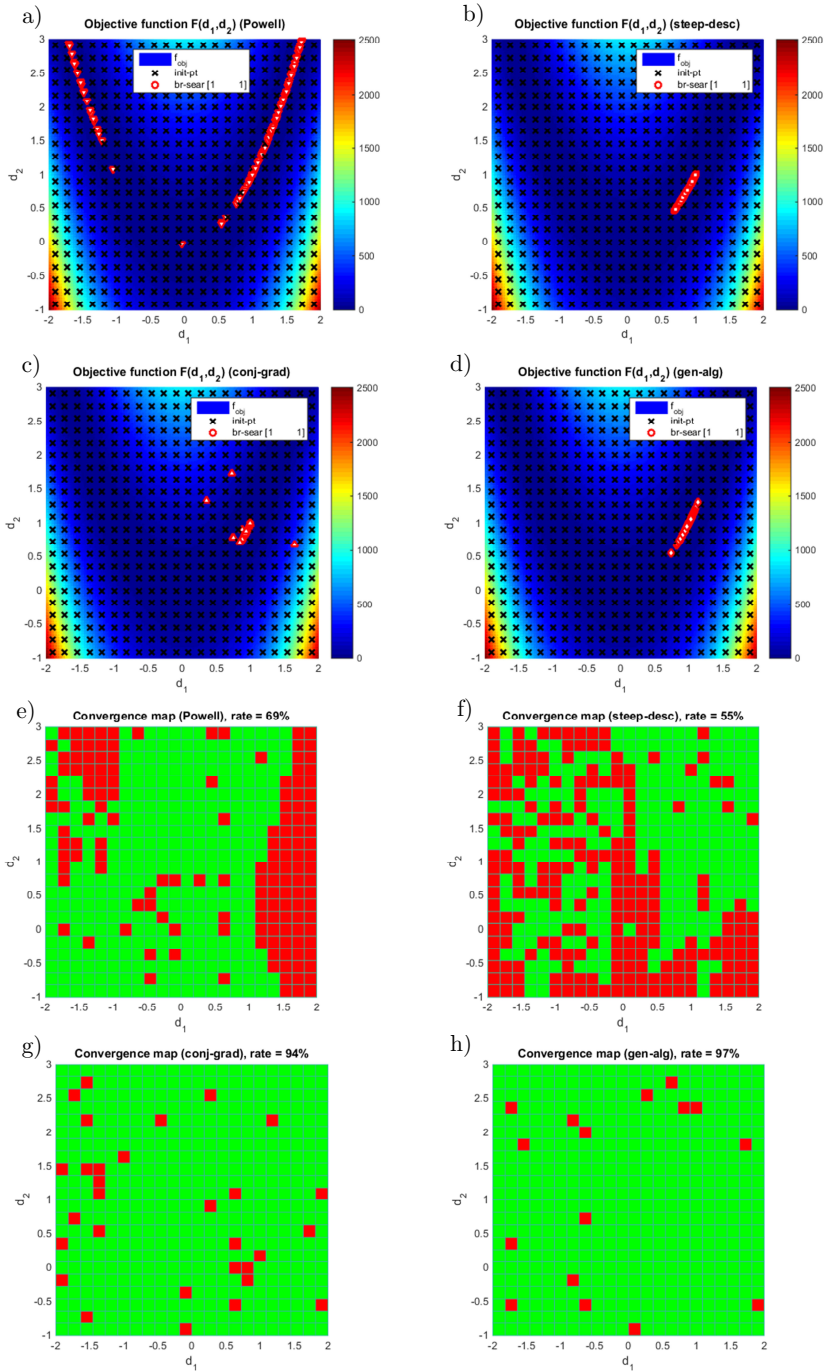


FIG. 6. Comparison of convergence maps for the Rosenbrock function for (a–e) Powell conjugate directions method, (b–f) steepest descent method, (c–g) conjugate gradients method, (d–h) genetic algorithms.

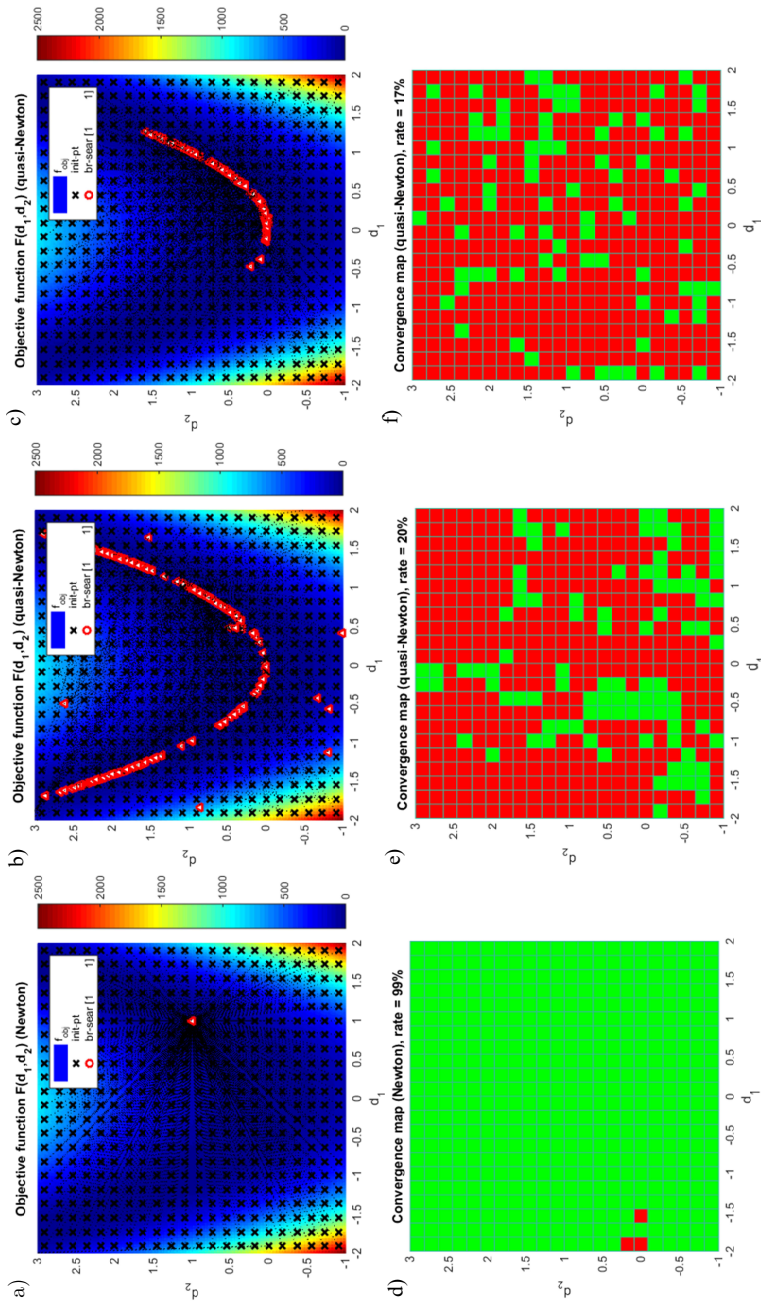


FIG. 7. Comparison of convergence maps for the Rosenbrock function for (a–d) Newton method with FD schemes, (b–e) quasi-Newton method with DFP formula, (c–f) quasi-Newton method with BFGS formula.

green fields related to the number of all fields (percentage values are displayed in the bottom graphs' titles of Fig. 6e–h and Fig. 7d–f).

One may notice that the Powell method is mostly convergent (Fig. 6a, e), though solutions are located inside the valley. On the other hand, the steepest descent method (Fig. 6b, f) produces more accurate solutions, though the solution convergence is very slow. Both conjugate gradients (Fig. 6c, g) and genetic algorithms (Fig. 6d, h) approaches have the highest convergence rates, though several solutions are improper. Eventually, convergence maps of the Newton method with FD schemes (Fig. 7a, d) are compared with quasi-Newton approaches with the most commonly applied formulas [35], namely Davidon-Fletcher-Powell (DFP) formula (Fig. 7b, e) and Broyden-Fletcher-Goldfarb-Shanno (BFGS) formula (Fig. 7c, f). In the case of both quasi-Newton approaches, many solutions are locked within the valley (similarly to the non-gradient Powell method), whereas nearly all starting points produce proper final solutions for the Newton method with FD schemes, being the variant proposed and applied in this research.

4.2. Preliminary results of multi-objective optimization

In this simple example, the goal is to present Pareto solutions along with the Pareto front for the most typical bar problems, including static, dynamic, and buckling scenarios. Furthermore, the characteristics of three variants of optimal solutions are discussed. A horizontal bar under a tensile uniform load with intensity $q_0 = 10^2$ kN/m and a compressive concentrated force P applied at the free end is considered. The bar material is characterized by the Young modulus $E = 10^6$ kPa and mass density $\rho = 8$ kg/m³. Its cross-sectional area is $A = 0.1$ h, where h is the cross-sectional height. The vector of decision variables consists of two ($n_d = 2$) parameters $\mathbf{d} = [h \ L]$, where $h \in [0.01 \ 0.1]$ m and $L \in [0.5 \ 5]$ m. Moreover, we deal with two ($n_f = 2$) optimization criteria $\mathbf{F}(\mathbf{d}) = [F_1(\mathbf{d}) \ F_2(\mathbf{d})]$, the second one of which corresponds to the total mass $F_2(\mathbf{d}) = bhL\rho$ of the structure, whereas the first one $F_1(\mathbf{d})$ depends on the problem type. Therefore, F_1 corresponds either to the maximum horizontal displacement (for $P = -10^3$ kN) for a static problem or to the inverse of the minimum natural frequency (for $P = 0$ and $q_0 = 0$) for an eigen dynamic problem (longitudinal vibrations) or to the inverse of the minimum critical force multiplier (for $P = \lambda$) for buckling analysis. The FE mesh consists of 10 elements of equal length.

Results obtained by means of a brute force search for a very densely divided admissible domain for decision variables, in aforementioned three various multi-objective optimization problems are presented in Fig. 8b–d, respectively. In each case, the entire Pareto-optimal set, being the result of a mapping between $\Omega_{\text{adm}} = [0.01 \ 0.1] \text{ m} \times [0.5 \ 5] \text{ m}$ and $\mathbf{F}(\Omega_{\text{adm}})$, is presented in a normalized

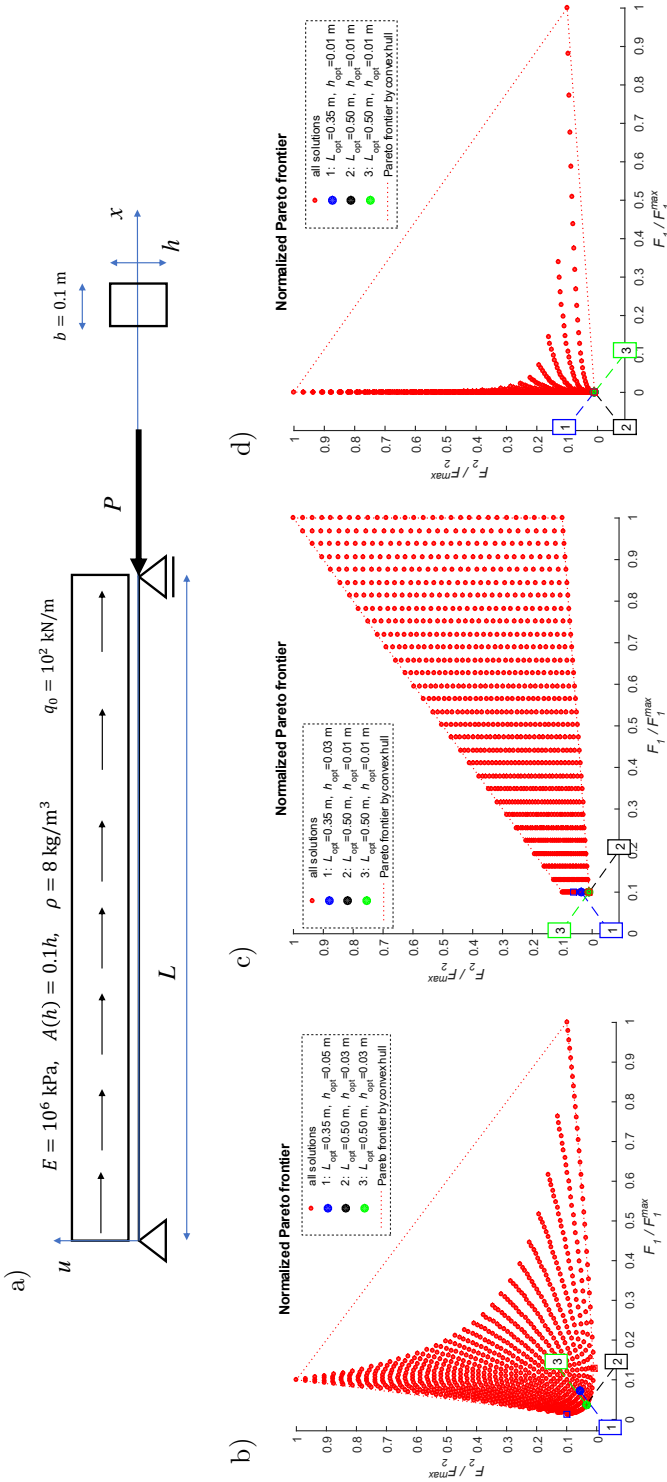


Fig. 8. Bar problem with two decision variables and two optimization criteria: a) mechanical model, b) Pareto front for static load, c) Pareto front for eigen dynamics, d) Pareto front for buckling problem.

(F_1, F_2) coordinate system. The efficient solutions located on Pareto-optimal front are indicated as well as its rough approximation by means of a convex hull. Finally, optimal solutions for h and L obtained from selected formulas including Eq. (2.12) (for unitary weights), Eq. (2.14) (for weights equal to the inverse of the largest value of the objective function, namely $\omega_l = (\max_{\mathbf{d}} F_l(\mathbf{d}))^{-1}$), and Eq. (2.15) (for unitary weights and $p = 2$) are displayed in the graphs' labels and marked. It may be observed that formulas (2.14) and (2.15) produce the same results in the form of non-dominated solutions located on the Pareto-optimal front, whereas the simplified formula (2.12) yields a dominated solution located inside the Pareto-optimal set.

4.3. Beam optimization

The objective of this example is to demonstrate the basic implementation of methods for a simple task involving the optimization of a beam with one or two decision variables. Brute force deflection and moment diagrams with one decision variable showcase how the location of maximum absolute values of moments and deflections, as well as the shape of deflection, change based on the support location. This example serves as a foundational demonstration of the optimization process and its impact on structural behavior. Two bending beam problems are considered: a beam under uniform load with intensity $q = 10 \text{ kN/m}$ (Fig. 9a) and a beam under trapezoidal load with intensity varying from $q_l = 10 \text{ kN/m}$ to $q_r = 40 \text{ kN/m}$ (Fig. 9b). In both load cases, a concentrated force $P = 10 \text{ kN}$ is applied at the right end. For the first case, only one decision variable is considered, which is the distance \mathbf{d}_r between the left and right supports, with the left support fixed. For the second case, the vector of decision variables consists of two parameters, namely $\mathbf{d} = [d_l \ d_r]$, where $d_l \in [0 \ 4.9] \text{ m}$ and $d_r \in [5.0 \ 10] \text{ m}$. Three optimization criteria are taken into account and formulated as follows: maximum deflection for the entire beam $F_1(\mathbf{d}) = \max_{(\xi)} |v(\mathbf{d}, \xi)|$, maximum moment for the whole beam $F_2(\mathbf{d}) = \max_{(\xi)} |M(\mathbf{d}, \xi)|$, and difference between support reactions $F_3(\mathbf{d}) = |R_l(\mathbf{d}) - R_r(\mathbf{d})|$.

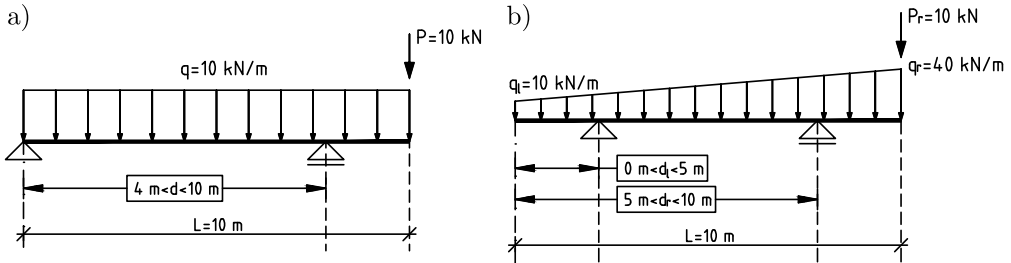


FIG. 9. Optimization problem of beams: one decision variable (a) and two decision variables (b).

Results for a one-dimensional ($n_d = 1$) optimization problem obtained by means of a brute force search with a Pareto front for two criteria are presented in Fig. 10. Results for a two-dimensional ($n_d = 2$) optimization problem obtained by means of a brute force are presented in Fig. 11a–c. Results for various starting points for selected criteria and various methods are presented in Fig. 12a–c.

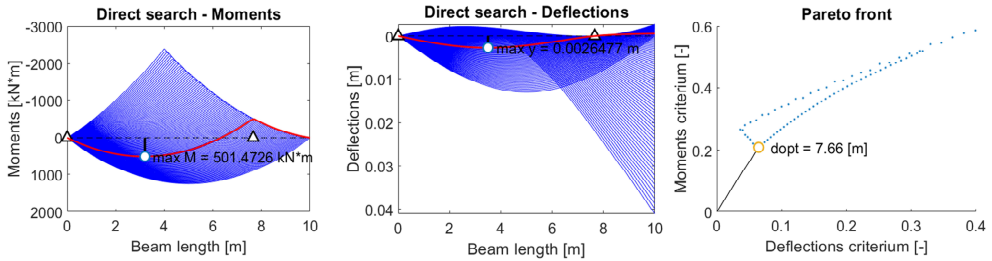


FIG. 10. Results of the beam optimization problem with one decision variable.

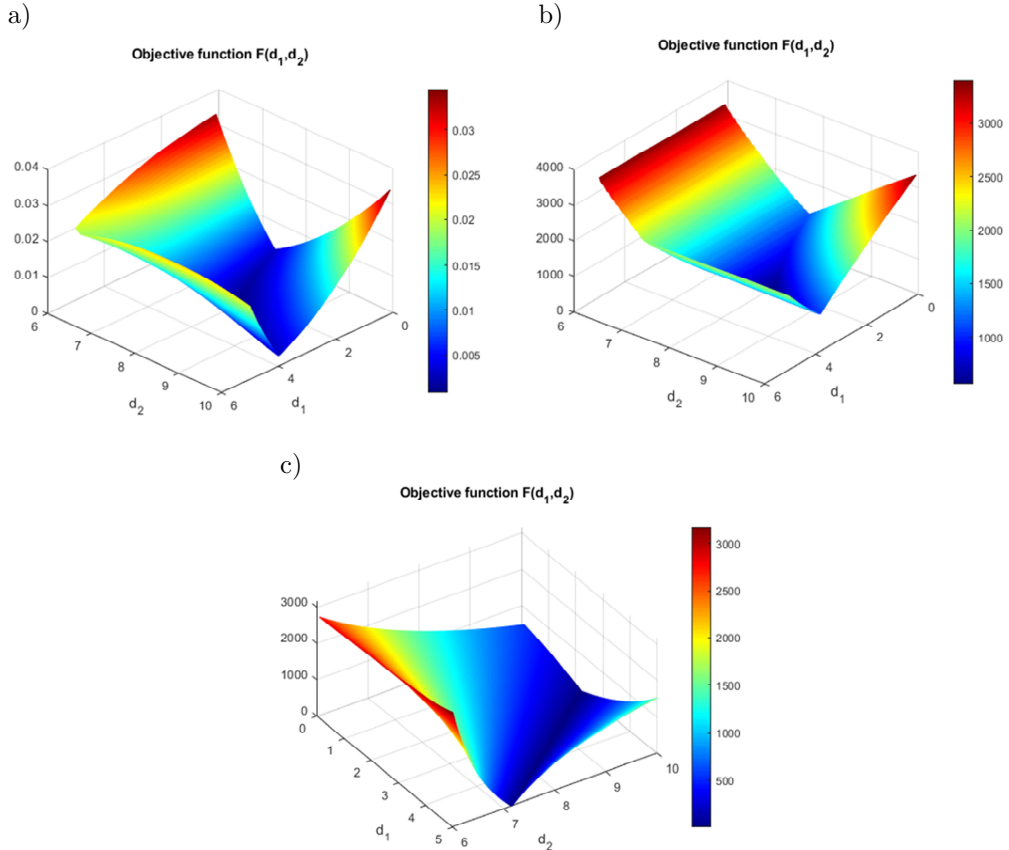


FIG. 11. Graphs of the objective functions for selected criteria:
 a) maximum deflections, b) maximum moments, c) difference between support reactions.

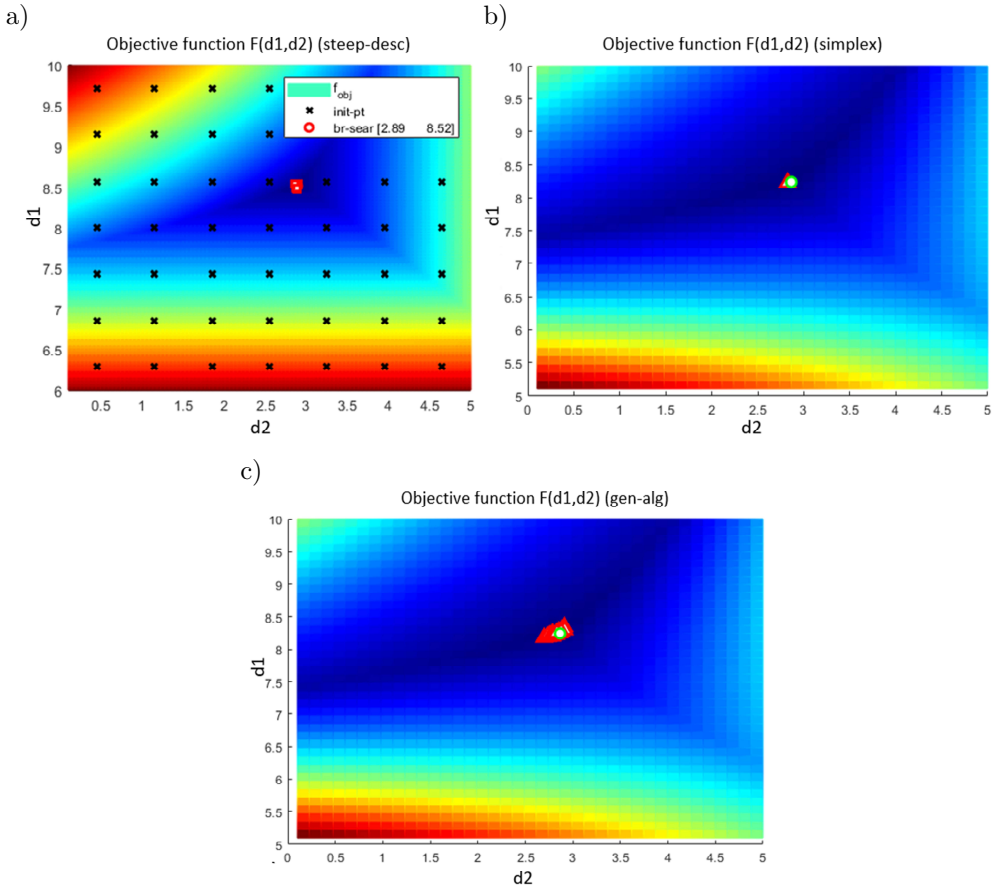


FIG. 12. Comparison of results for various starting points for deflection criterion:
 a) steepest descent method, b) Nelder-Mead simplex, c) genetic algorithms.

4.4. Truss optimization

The objective of this example is to apply the proposed pattern approach to basic truss structures characterized by typical engineering parameters such as cross-sections and truss widths. Testing singular truss patterns is vital before integrating them with other patterns. This step ensures that individual patterns function correctly and lays the groundwork for their integration into more complex structural configurations involving multiple patterns. Two types of trusses are considered: a vertical truss subjected to concentrated vertical $F_z = -250$ kN and horizontal $F_x = 50$ kN forces (Fig. 13a), as well as a horizontal truss under trapezoidal load with intensity varying from $q_l = 30$ kN/m to $q_r = 10$ kN/m (Fig. 13b). Two decision variables are taken into account, hence $\mathbf{d} = [d_1 \ d_2]$. For the vertical truss, the width of the truss $d_1 \in [1 \ 4.5]$ m

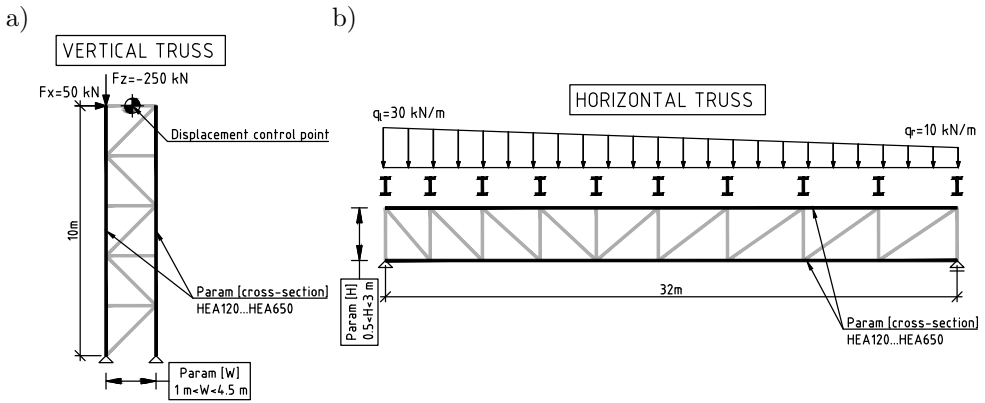


FIG. 13. Optimization problem of trusses.

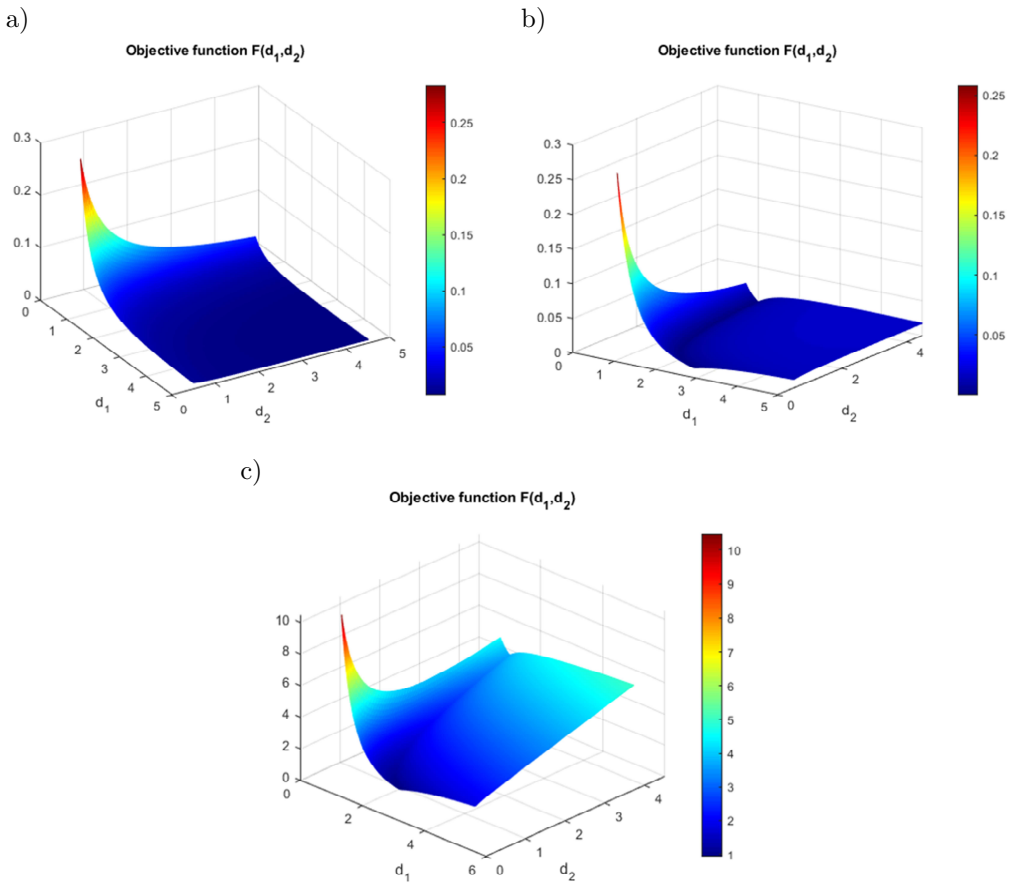


FIG. 14. Graphs of objective functions for the vertical truss with selected criteria: a) horizontal displacement of the control node, b) displacement limitation $H/400$, c) displacement limitation $H/400 +$ steel usage (weighted).

and the area of the cross-section of chords $d_2 \in [0.1 \ 0.4] \text{ m}^2$. For the horizontal truss, the height of the truss $d_1 \in [0.5 \ 3] \text{ m}$ and the area of the cross-section of chords $d_2 \in [0.1 \ 0.7] \text{ m}^2$. Three optimization criteria are considered and formulated as follows: displacement in the control node (horizontal displacement for vertical truss $F_1(\mathbf{d}) = h(\mathbf{d})$ and vertical displacement for horizontal truss $F_1(\mathbf{d}) = v(\mathbf{d})$), displacement limitation as the difference between displacement in the control node and admissible displacement $F_2(\mathbf{d}) = |h(\mathbf{d}) - h_{\text{adm}}|$, $F_2(\mathbf{d}) = |v(\mathbf{d}) - v_{\text{adm}}|$, $v_{\text{adm}} = L/250$, $h_{\text{adm}} = H/400$ (where L is the span of the horizontal truss and H is the height of the vertical truss), and steel usage as the total volume of bars $F_3(\mathbf{d}) = A(\mathbf{d})l(\mathbf{d})\rho$.

Results for a two-dimensional ($n_d = 2$) optimization problem obtained by means of a brute force are presented in Fig. 14a–c and Fig. 15a–c for vertical and horizontal trusses, respectively. Additionally, results obtained for various starting points as well as selected criteria and methods are presented in Fig. 16a–c.

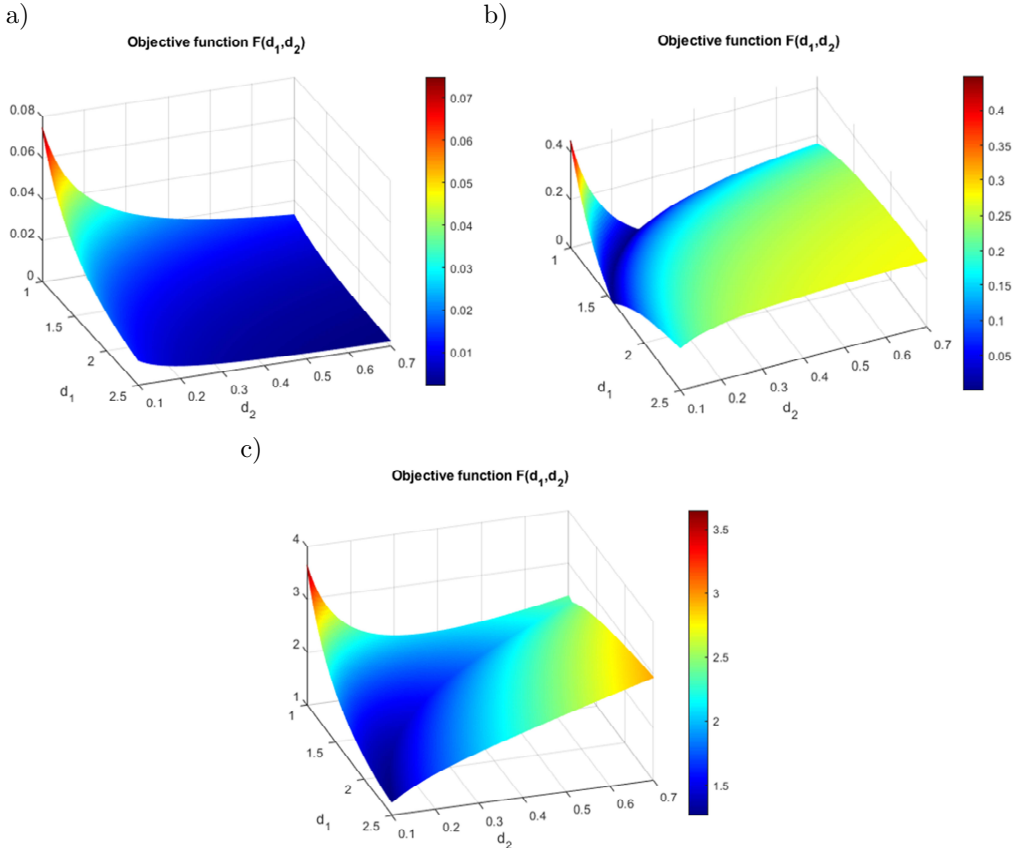


FIG. 15. Graphs of objective functions for horizontal truss with selected criteria: a) vertical displacement of the control node, b) displacement limitation $L/250$, c) displacement limitation $L/250 +$ steel usage (weighted).

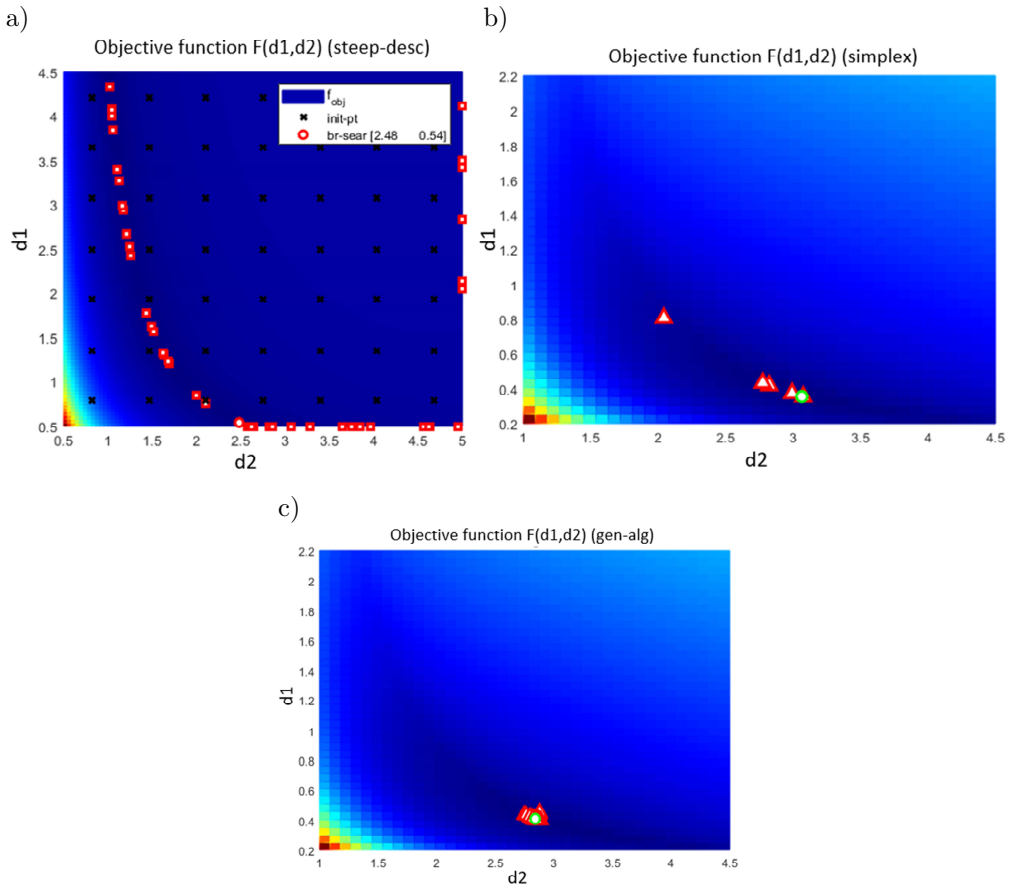


FIG. 16. Comparison of results for various starting points for a displacement limitation criterion $H/400$: a) steepest descent method, b) Nelder-Mead simplex, c) genetic algorithm.

4.5. Beam grid optimization

A beam grid is a pattern designed to optimize secondary beams or purlins in a plane. The optimization process for the pattern consists of two stages:

- 1) Pre-processing, where the algorithm adjusts beam spacing in accordance with the shape of the loading to ensure an equal value of loading for each beam (Fig. 17).
- 2) Optimization based on selected criteria.

At the first stage, the algorithm provides proportional coefficients for beam spacing in each zone to ensure equal load distribution. These coefficients relate to a single parameter for the beam spacing (averaged beam spacing for the entire pattern) which is then subjected to optimization. The task is aimed at optimization with two decision variables $\mathbf{d} = [d_1 \ d_2]$, namely the cross-section

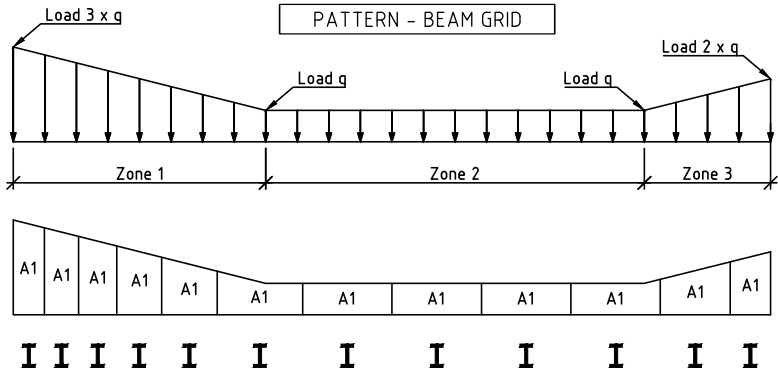


FIG. 17. Optimization problem of a beam grid.

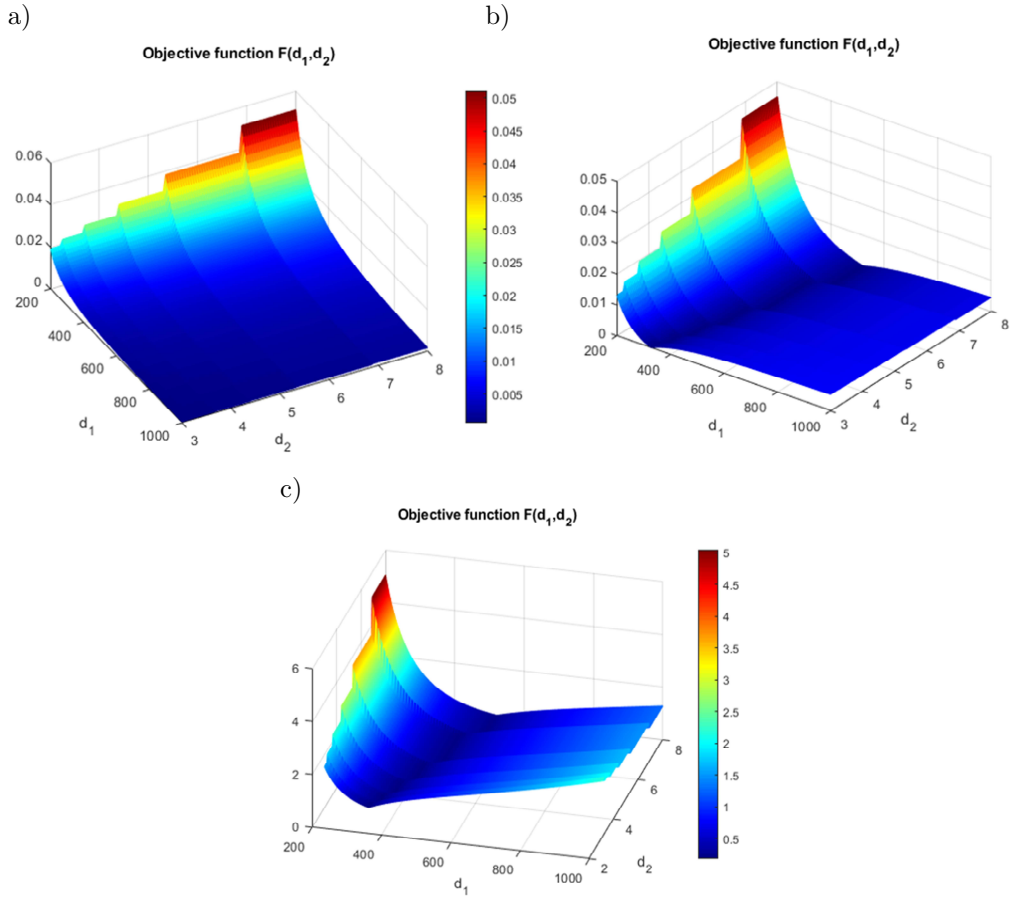


FIG. 18. Graphs of objective functions for beam grids with selected criteria: a) beams deflection, b) deflection limitation criterion $L/250$, c) deflection limitation criterion $L/250$ + steel usage (weighted).

height $d_1 \in [200 \ 1000]$ mm and the averaged beam spacing $d_2 \in [3 \ 8]$ m. Cross-sections properties are calculated based on the cross-section height d_1 and profile geometry from the selected catalogue (HEA profiles) with approximation of table values. Table values were approximated for the purpose of implementation of the gradient optimization methods. Three optimization criteria are considered: beams deflection $F_1(\mathbf{d}) = v(\mathbf{d})$, deflection limitation as the difference between calculated beam deflection and admissible deflection $F_2(\mathbf{d}) = |v(\mathbf{d}) - v_{\text{adm}}|$, $v_{\text{adm}} = L/250$ (where L is the span of the beams), and steel usage as the total volume of beams $F_3(\mathbf{d}) = A(\mathbf{d})l\rho$. Values of deflections are obtained analytically. For benchmark purposes, a trapezoidal load with intensity varying from $q_l = 30$ kN/m to $q_r = 10$ kN/m is taken into account.

Results for a two-dimensional optimization problem obtained by means of brute force are presented in Fig. 18a–c. Additionally, results for selected starting points, criteria and methods are presented in Fig. 19a–c. The particular stepped

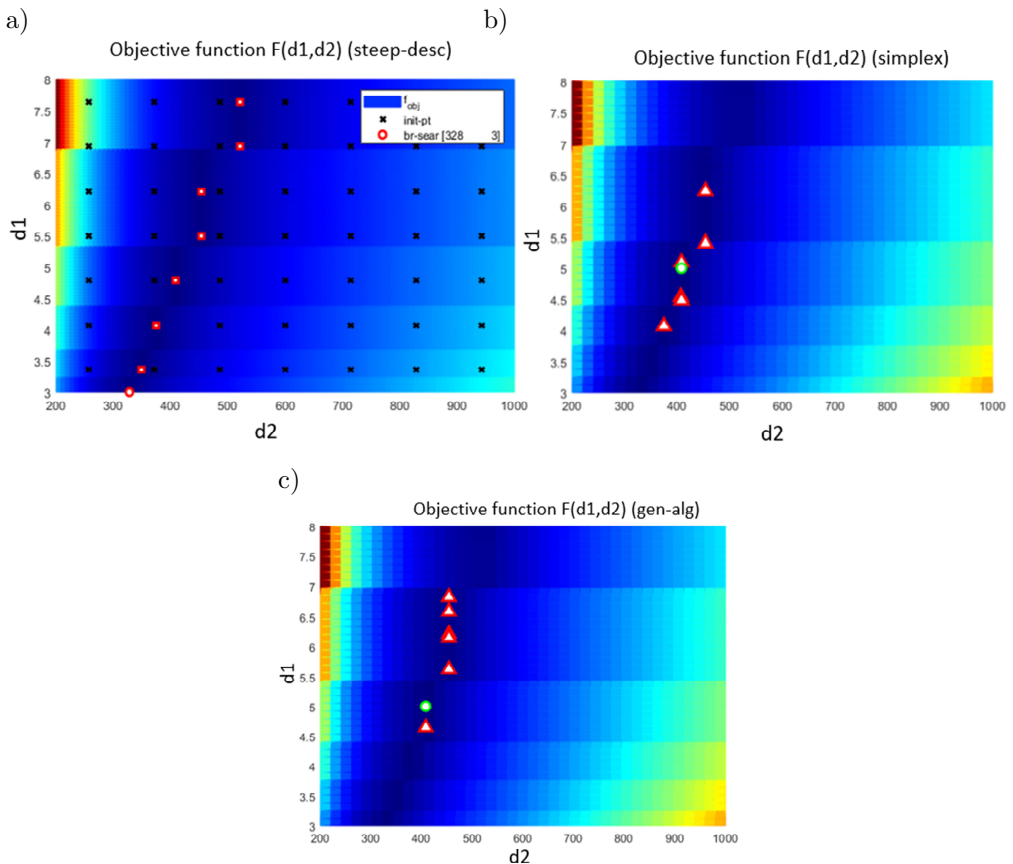


FIG. 19. Comparison of results for various starting points for a mixed criterion (deflection limitation $L/250$ and steel usage): a) steepest descent method, b) Nelder-Mead simplex, c) genetic algorithms.

shape of the objective function is related to the beam spacing parameter. During optimization, the beam spacings (real numbers) are converted to the number of purlins (integer value). For the purpose of optimization, local smoothing, built-in in FD schemes is applied for gradient-based methods.

4.6. Combination of patterns

The concept of patterns involves the integration of individual patterns into a complex structure (Fig. 20a). For preliminary research, a connection between three basic patterns is considered: a beam grid, a horizontal truss, and two vertical trusses. Sequential optimization, starting from roof purlins to vertical trusses, is assumed following the general algorithm (Fig. 20b).

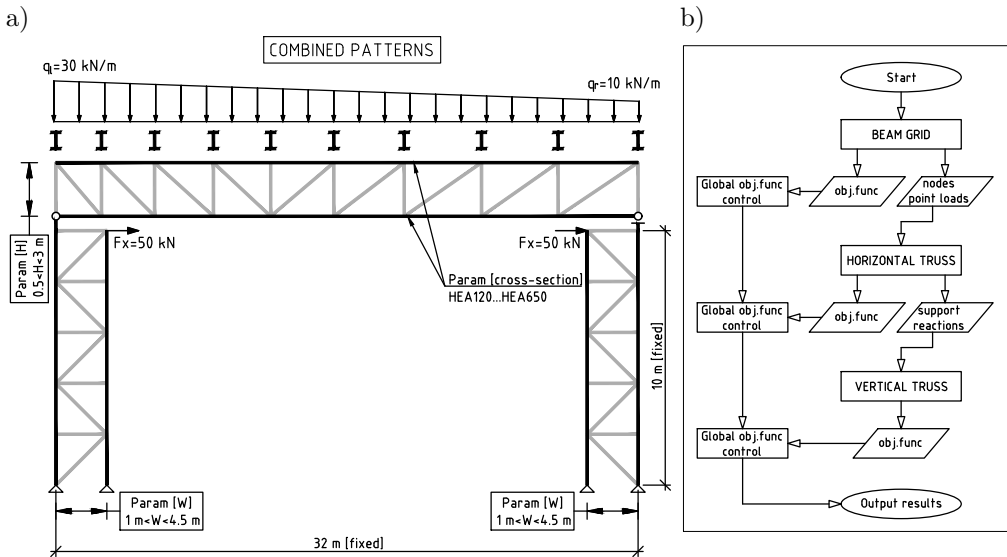


FIG. 20. Preliminary concept of a combination of several patterns: a) general layout of the structure, b) general flow chart of sequential optimization.

The key advantage of this approach is the ability to control global objective function values, such as the total weight of the entire structure, for each specific pattern during optimization. The optimization process yields the objective function values for each pattern and allows to take into account the contribution of each pattern with formulation of the global objective function \mathbf{F}_{tot} , namely $\mathbf{F}_{\text{tot}} = \sum_{i=1}^{n_p} \mathbf{F}_i$, where n_p is the total number of patterns (here $n_p = 4$). This analysis is crucial for evaluating the total costs of steel prefabrication, which may include factors beyond the total weight of steel, such as the number of elements and joints. A larger number of elements and joints increases the complexity

of production. For selected combination of four patterns, the global objective function \mathbf{F}_{tot} is a three-valued vector function whose components correspond to optimization criteria related to the total weight of the entire structure, the total number of elements and the total number of joints. This approach enables a influence analysis of each pattern at the global scale, as depicted in Fig. 21.

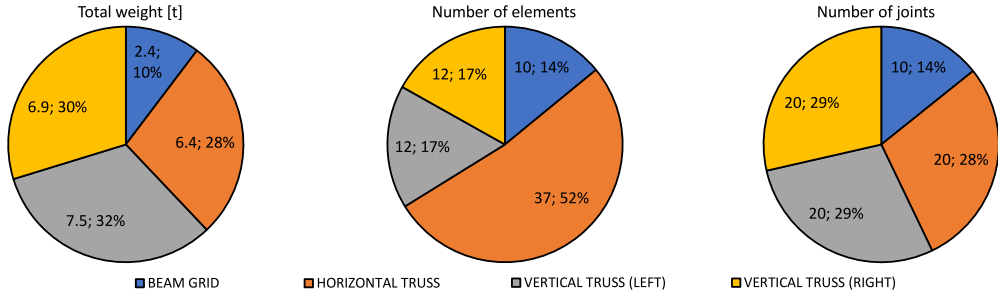


FIG. 21. Summary of optimization results for a combination of patterns taking into consideration: total weight of the structure, number of elements and number of joints.

In this specific example, it is observed that the beam grid pattern contributes the least to the total weight of the structure. However, optimizing the beam grid may lead to a larger number of joints in the horizontal truss. Considering that the beam grid pattern is directly connected to nodes of the horizontal truss, this increases the number of braces and, consequently, the total weight of the structure. This preliminary approach holds promise due to the numerous possibilities for combining various structural patterns for different applications. Indeed, allowing for modifications to the general algorithm provides greater flexibility and control over patterns during optimization. By adjusting the sequence of optimization steps or introducing additional parameters, researchers can explore various optimization strategies and potentially achieve different results. This avenue of investigation opens up opportunities for further research and experimentation in the field.

4.7. Structural reliability estimation

In all the previously discussed engineering examples, the parameters of the subjected load were assigned fixed and unambiguous values. Consequently, one optimal solution was obtained from the family of possible solutions using parametric description and the relevant optimization algorithm. However, a more general and complex scenario may involve uncertainty inherent in selected load parameters. If these parameters are modeled as probabilistic variables, we deal with structural reliability, denoted as R_s . Structural reliability serves as a probabilistic measure of structural safety [41]. It is defined as the probability of

the complement of failure (or the probability of the occurrence of the inverse event to the failure). Failure in this context happens when the total applied load exceeds the total resistance of the structure, represented, for instance, by exceeding its maximum admissible displacement, a scenario considered in this research. The primary objective of this example is to evaluate the developed optimization algorithm, which integrates the FEM with the Newton method using Finite Difference schemes. This approach is applied to solve numerous beam optimization problems under different load configurations in a fast and accurate manner. Moreover, stochastic methods, commonly used in descriptive statistics, are employed to determine the optimal location of supports to ensure maximal structural reliability. Afterward, the final reliability of the determined beam geometry is estimated.

Consider a bending problem with two decision variables as introduced in 4.3. The steel beam structure with a total length of $L = 5$ m, cross-section dimensions of $0.1 \text{ m} \times 0.2 \text{ m}$, and Young's modulus $E = 210 \text{ GPa}$ is subjected to a uniform load with a fixed intensity $q_0 = 60 \text{ kN/m}$, as well as to a concentrated force P_0 located at x_0 . The structure pattern is modeled using a parametric description such that variable locations of both supports $d_l \in [0, 2.23] \text{ m}$ and $d_r \in [2.53, 5] \text{ m}$ generate the entire family of possible structures. The primary objective is to determine optimal locations d_l^{opt} and d_r^{opt} of supports to ensure the maximum possible reliability of the beam. Assuming that the probability of load density and structure resistance are denoted as $p(s)$ and $r(s)$ respectively, where s is the random variable corresponding to the uncertain load parameter, reliability can be analytically determined if both p and r are normal (Gaussian) distributions. However, in most cases, load and resistance are not normally distributed and explicitly formulated. Moreover, the admissible domain Ω_{adm} of safety load states is a priori unknown. Therefore, an appropriate numerical approach is required, usually by means of a Monte Carlo simulation and the stripes method [42, 43].

The entire area below the graph of p is divided into a large number K of bars of equal base B and heights $H_k = p((k - 1)h + 0.5h)$, $k = 1, 2, \dots, K$. Subsequently, a series of simulations are performed, each time selecting a random number $r \in (0, 1)$ and determining the smallest k_0 for which $B \sum_{k=1}^{k_0} H_k \geq r$. Afterwards, the mechanical problem is solved by the finite element (FE) framework, assuming temporarily fixed load parameter(s) corresponding to $s_0 = (1 - k_0)h + 0.5h$.

Two variants may be distinguished. In case supports locations d_l and d_r are fixed (no geometry optimization), the safety condition is examined, namely $v_{\text{max}} < v_{\text{adm}} = L/500 = 10 \text{ mm}$, where v_{max} is the maximum beam deflection, and the admissible deflection $v_{\text{adm}} = L/500$ corresponds to Eurocode sustain-

ability condition for primary steel beams. The number of admissible states is counted, while the final reliability may be estimated as follows:

$$(4.2) \quad R_s = \int_{\Omega_{\text{adm}}} p(s) \, ds \approx \frac{N_{\text{adm}}}{N_{\text{tot}}},$$

where N_{adm} is the number of admissible states and N_{tot} is the number of all Monte Carlo simulations. Certainly, Monte Carlo estimation combined with the strap method offers an approximate means of determining the admissible domain Ω_{adm} . In practical computations, it is convenient to express R_s using the reliability index β , which corresponds to the failure probability $R_f = 1 - R_s$. When both the load and resistance follow normal distributions and are uncorrelated, the Cornell reliability index can be utilized. In a more general scenario, the Hasofer-Lind reliability index is employed [44]. This index is defined as the minimum distance between the limit state surface, which serves as the boundary $\Gamma_{sf} = \Omega_{\text{adm}} \cap \Omega_{\text{fail}}$ between the admissible Ω_{adm} and failure Ω_{fail} domains, and the origin of the coordinate system of normalized random variables.

In the second variant, support locations d_l and d_r have to be optimally determined for each randomly selected load parameter(s) using, for instance, a fast and accurate Newton method with FD schemes proposed in this paper. The statistical distribution of optimal support locations has to be determined (e.g., using histograms). Eventually, the stochastic family of optimal support locations is represented by means of center (mean, mode, median), dispersion, or shape parameters yielding one set of d_l^{opt} and d_r^{opt} compromising all possible load parameter distribution(s) and the variance of support locations. The final structural reliability is determined using the methodology outlined for the first variant. It suffers from the total error accumulating errors of the stripes method ($\varepsilon \leq 1/K$), Monte Carlo approach ($\varepsilon \leq 1/\sqrt{N_{\text{tot}}}$), and optimization method ($\varepsilon \leq \varepsilon_d$). Discretization and approximation errors are negligible.

First, we assume a fixed concentrated force magnitude $P_0 = 100$ kN, whereas the force location x_0 is ascribed by the normal Gauss distribution with a mean value $\mu = 2.5$ m and a standard deviation $\sigma = 0.63$ m, as shown in Fig. 22a. The number of stripes is set to $K = 10^2$, and the total number of Monte Carlo simulations is $N_{\text{tot}} = 10^3$. Results of reliability estimation and admissible domains for three specified and typical support locations (without automatic optimization) are shown in Fig. 23a (external locations $d_l = 0$ and $d_r = 5$ m), in Fig. 23b (middle locations $d_l = 0.83$ m and $d_r = 4.17$ m), and in Fig. 23c (internal locations $d_l = 2.02$ m and $d_r = 3.02$ m). The fuzziness of reliability is significant as it varies from 0% to 58% (with $\beta = 0.19$ only), each time yielding completely different borders of the admissible interval (marked in green). Therefore, fully justified geometry optimization is performed, and an approximate stochastic

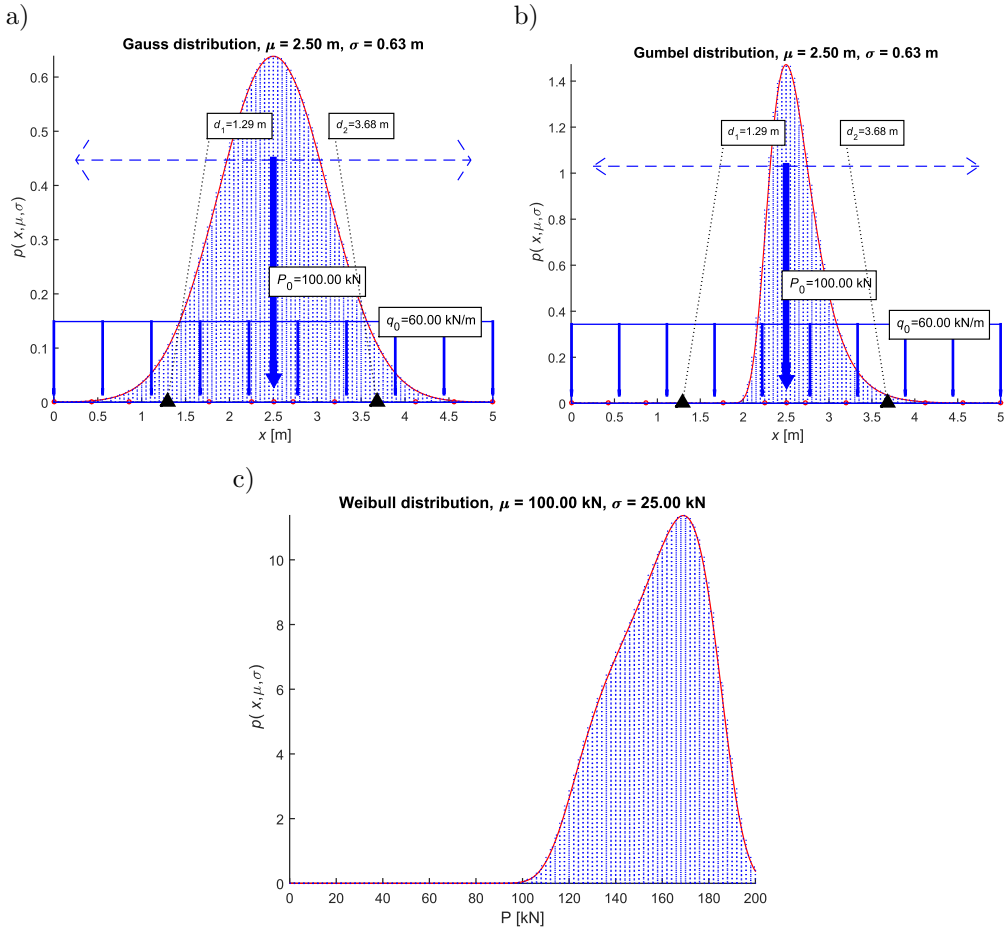


FIG. 22. Probability distributions for force location x_0 : a) Gauss distribution, b) Gumbel distribution and force magnitude P_0 , c) Weibull distribution.

representation of the distribution of both support locations in the form of histograms is presented in Fig. 23d,e. On this basis, mean values of $d_l^{\text{opt}} = 1.27$ m and $d_r^{\text{opt}} = 3.73$ m are accepted as the optimal ones, and the final reliability analysis is performed yielding results shown in Fig. 23f with successfully maximized $R_s = 99.80\%$ (with $\beta = 2.76$), and an admissible interval covering almost the entire problem domain.

A similar study is conducted for two uncertain load parameters, namely a force location x_0 (Gumbel distribution with $\mu = 2.5$ m and $\sigma = 0.63$ m – Fig. 22b) and force magnitude (Weibull distribution with $\mu = 100$ kN and $\sigma = 25$ kN – Fig. 22c). In contrast to normal distribution, which is typically used for modeling an unknown mean value representing the entire population, Gumbel

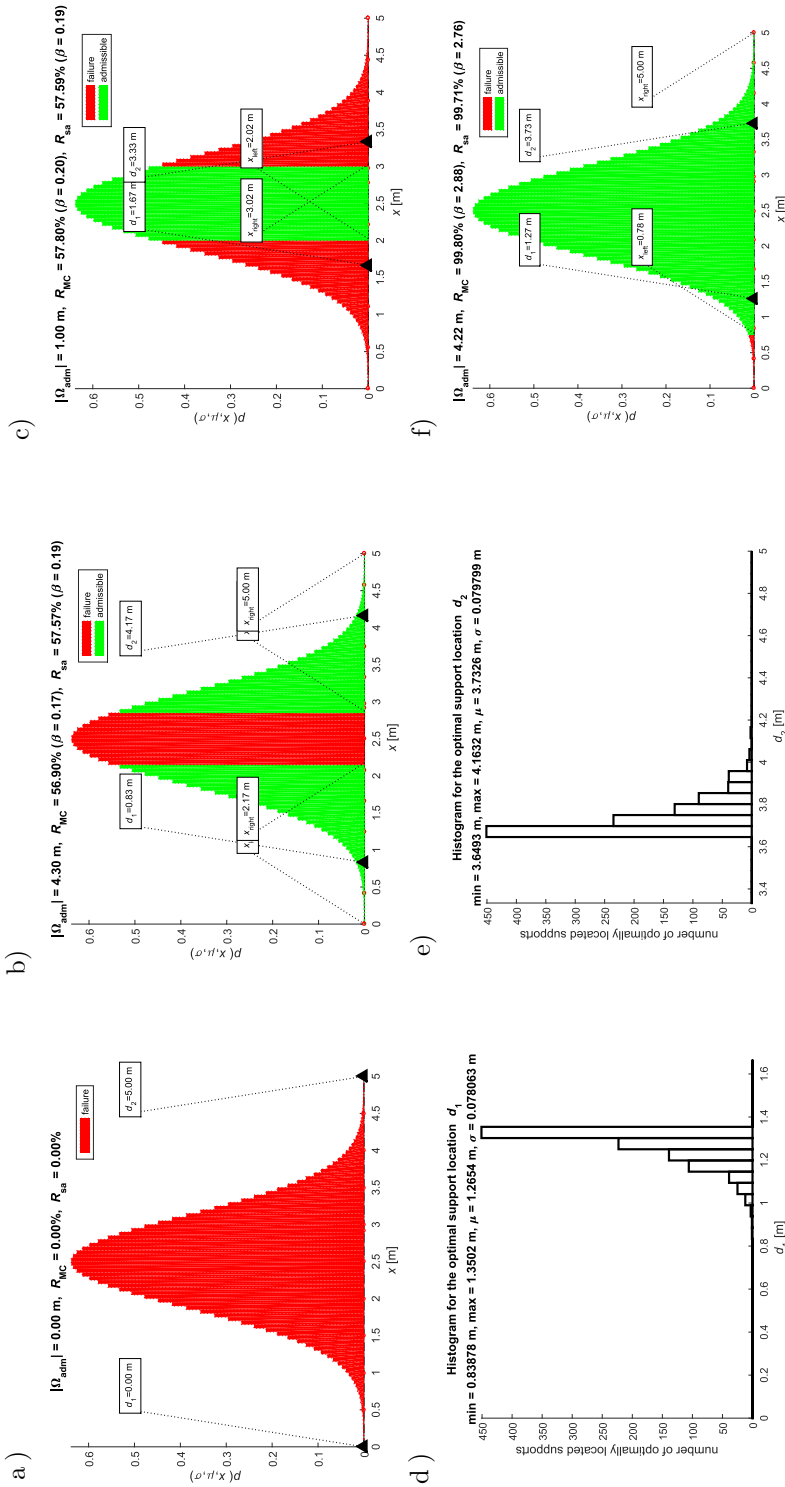


FIG. 23. Results for the reliability estimation for fixed force magnitude P_0 and uncertain force location x_0 : a–c) reliability estimations and admissible intervals for three typical support locations, d) and e) histograms of optimal support locations, f) reliability estimation and admissible interval for mean optimal locations.

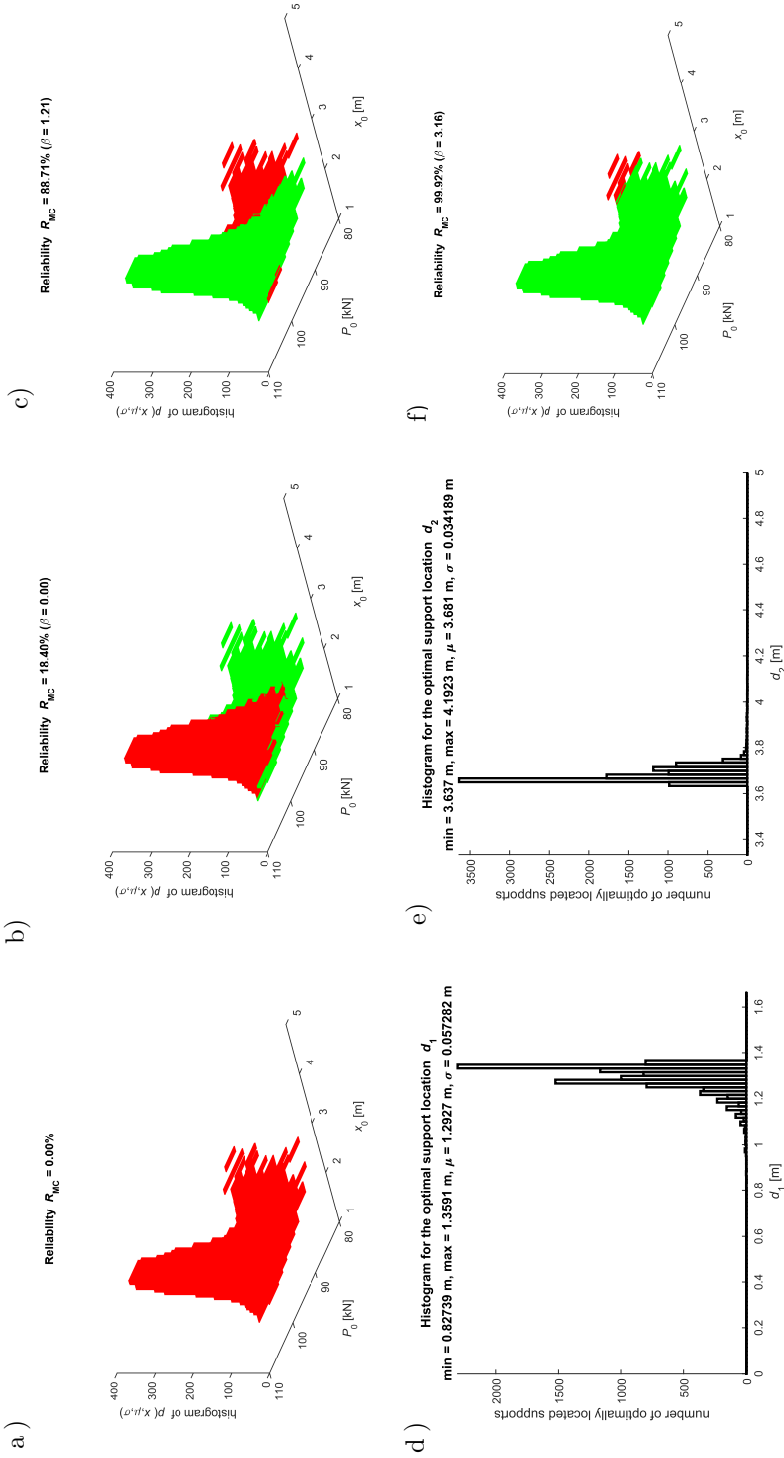


FIG. 24. Results for the reliability estimation for uncertain force magnitude P_0 and force location x_0 : a-c) reliability estimations and admissible domains for three typical support locations, d) and e) histograms of optimal support locations, f) reliability estimation and admissible domain for mean optimal locations.

and Weibull distributions are usually applied for extreme and time-dependent values, respectively. Final results of reliability analysis (for $K = 10^2$ and with an increased $N_{\text{tot}} = 10^4$) are presented in Fig. 24 in the same fashion as previously. 2D bar graphs in Fig. 24a–c indicate a large dispersion of reliability (from 0% to 89%, yielding maximal $\beta = 1.21$ only) as well as sensitivity of the safety domain (green regions) to selected support locations (same as above). In Fig. 24d,e, stochastic optimization results of support locations are shown. Consequently, for their mean values $d_l^{\text{opt}} = 1.29$ m and $d_r^{\text{opt}} = 3.68$ m, the optimized structural reliability reaches $R_s = 99.92\%$ ($\beta = 3.16$) – see Fig. 24f. The entire process requires 4 minutes of an Intel Core CPU with 1.8 GHz and 16 GB RAM, whereas other optimization approaches, including brute force search, would need more than 2 hours.

5. CONCLUSIONS

A numerical approach to geometry and size engineering optimization problems is presented. The main concept involves decomposing the complex steel bar structure into several typical patterns, each with a reduced number of decision variables. Such a move allows for effective and fast solution of local optimization problems corresponding to those structural patterns (e.g., beam, horizontal and vertical trusses) followed by the relevant interactions between them. We have formulated the multi-dimensional and multi-criteria optimization problem and we proposed three variants incorporating set of single-objective problems. The single-objective optimization problem may be tackled by improved deterministic approaches, especially those of gradient nature. In this case, determination of the objective function gradient (and Hessian) is achieved by means of appropriate finite difference schemes rather than standard techniques using consecutive solution approximations. Furthermore, a consistent and divergence-free bisection approach is employed to evaluate the step size for both non-gradient and gradient methods. A particularly convenient approach appears to be a new version of the Newton method that utilizes both finite element (FE) and finite difference (FD) frameworks. A variety of benchmark tests and engineering problems were examined. Special emphasis was placed on issues where a large number of small optimization problems have to be solved in a fast and accurate manner, including mutual cooperation between patterns as well as problems involving uncertain load parameters.

While the obtained results are promising, this research – the culmination of a one-year implementation PhD – is still under development, and there is much work yet to be done. The next step in our investigation involves exploring combinations of a larger number of patterns, each with an increased number of decision variables. Estimating structural reliability while simultaneously opti-

mizing design parameters is another promising and intriguing avenue for future research, particularly in cases where larger values of reliability indices are anticipated (e.g., for ultimate limit states). Therefore, replacing the Monte Carlo approach with a more sophisticated numerical framework will be necessary to effectively handle probabilities with higher resolution. Furthermore, we plan to consider more complex truss and frame problems with non-linearities of the second (geometry stiffness) and the third (large deformations) orders as well as thermo-mechanical coupling and the impact of exceptional loading conditions on structures.

ACKNOWLEDGMENTS

The research is supported by the Polish Ministry of Science and Higher Education under the project DWD/6/0523/2022 “Parameterization of computational models with topology optimization of selected types of building structures”.

REFERENCES

1. ROZVANY G.I.N., Aims, scope, methods, history and unified terminology of computer aided topology optimization in structural mechanics, *Structural and Multidisciplinary Optimization*, **21**(2): 90–108, 2001, doi: 10.1007/s001580050174.
2. ROZVANY G.I.N., A critical review of established methods of structural topology optimization, *Structural and Multidisciplinary Optimization*, **37**(3): 217–237, 2009, doi: 10.1007/s00158-007-0217-0.
3. SIGMUND O., MAUTE K., Topology optimization approaches, *Structural and Multidisciplinary Optimization*, **48**(6): 1031–1055, 2013, doi: 10.1007/s00158-013-0978-6.
4. DUNNING P.D., On the co-rotational method for geometrically nonlinear topology optimization, *Structural and Multidisciplinary Optimization*, **62**(5): 2357–2374, 2020, doi: 10.1007/s00158-020-02605-4.
5. WANG W., FENG D., YANG L., LI S., WANG C.C., Topology optimization of self-supporting lattice structure, *Additive Manufacturing*, **67**: 103507, 2023, doi: 10.1016/j.addma.2023.103507.
6. WANG B., BAI J., LU S., ZUO W., Structural topology optimization considering geometrical and load nonlinearities, *Computers and Structures*, **289**: 107190, 2023, doi: 10.1016/j.compstruc.2023.107190.
7. ZHANG L., ZHANG Y., VAN KEULEN F., Topology optimization of geometrically nonlinear structures using reduced-order modeling, *Computer Methods in Applied Mechanics and Engineering*, **416**: 116371, 2023, doi: 10.1016/j.cma.2023.116371.
8. LIU Y., GAO R., LI Y., FANG D., EMsFEM based concurrent topology optimization method for hierarchical structure with multiple substructures, *Computer Methods in Applied Mechanics and Engineering*, **418**: 116549, 2024, doi: 10.1016/j.cma.2023.116549.

9. CHRISTENSEN C.F., WANG F., SIGMUND O., Topology optimization of multiscale structures considering local and global buckling response, *Computer Methods in Applied Mechanics and Engineering*, **408**: 115969, 2023, doi: 10.1016/j.cma.2023.115969.
10. MOVAHEDI RAD M., HABASHNEH M., LÓGÓ J., Reliability based bi-directional evolutionary topology optimization of geometric and material nonlinear analysis with imperfections, *Computers and Structures*, **287**: 107120, 2023, doi: 10.1016/j.compstruc.2023.107120.
11. FREITAG S., PETERS S., EDLER P., MESCHKE G., Reliability-based optimization of structural topologies using artificial neural networks, *Probabilistic Engineering Mechanics*, **70**: 103356, 2022, doi: 10.1016/j.probenmech.2022.103356.
12. YU Y., WEI M., YU J., CUI Y., GAO R., DONG Z., WANG X., Reliability-based design method for marine structures combining topology, shape, and size optimization, *Ocean Engineering*, **286**: 115490, 2023, doi: 10.1016/j.oceaneng.2023.115490.
13. TRAN Q.D., SHIN D., JANG G.W., Bayesian optimization-based topology optimization using moving morphable bars for flexible structure design problems, *Engineering Structures*, **300**: 117103, 2024, doi: 10.1016/j.engstruct.2023.117103.
14. YAN F., LIN Z., WANG X., AZARMI F., SOBOLEV K., Evaluation and prediction of bond strength of GFRP-bar reinforced concrete using artificial neural network optimized with genetic algorithm, *Composite Structures*, **161**: 441–452, 2017, doi: 10.1016/j.compstruct.2016.11.068.
15. SONMEZ M., Discrete optimum design of truss structures using artificial bee colony algorithm, *Structural and Multidisciplinary Optimization*, **43**(1): 85–97, 2011, doi: 10.1007/s00158-010-0551-5.
16. FREDRICKSON H., Topology optimization of frame structures – joint penalty and material selection, *Structural and Multidisciplinary Optimization*, **30**(3): 193–200, 2005, doi: 10.1007/s00158-005-0515-3.
17. CAI J., HUANG L., WU H., YIN L., Topology optimization of truss structure under load uncertainty with gradient-free proportional topology optimization method, *Structures*, **58**: 105377, 2023, doi: 10.1016/j.istruc.2023.105377.
18. GUO X., CHENG G.D., OLHOFF N., Optimum design of truss topology under buckling constraints, *Structural and Multidisciplinary Optimization*, **30**(3): 169–180, 2005, doi: 10.1007/s00158-004-0511-z.
19. BEN-TAL A., BENDSOE M.P., A new method for optimal truss topology design, *SIAM Journal on Optimization*, **3**(2): 322–358, 1993, doi: 10.1137/0803015.
20. AWAD R., Sizing optimization of truss structures using the political optimizer (PO) algorithm, *Structures*, **33**: 4871–4894, 2021, doi: 10.1016/j.istruc.2021.07.027.
21. STOLPE M., Truss optimization with discrete design variables: a critical review, *Structural and Multidisciplinary Optimization*, **53**(2): 349–374, 2016, doi: 10.1007/s00158-015-1333-x.
22. ACHTZIGER W., STOLPE M., Truss topology optimization with discrete design variables – Guaranteed global optimality and benchmark examples, *Structural and Multidisciplinary Optimization*, **34**(1): 1–20, 2007, doi: 10.1007/s00158-006-0074-2.
23. DILLEN W., LOMBAERT G., SCHEVENELS M., A hybrid gradient-based/metaheuristic method for Eurocode-compliant size, shape and topology optimization of steel structures, *Engineering Structures*, **239**: 112137, 2021, doi: 10.1016/j.engstruct.2021.112137.

24. BOJCZUK D., RĘBOSZ A., Topology optimisation of trusses using bars exchange method, *Bulletin of the Polish Academy of Sciences, Technical Sciences*, 2012, doi: 10.2478/v10175-012-0025-6.
25. KALITA K., CHOCHAN J.S., JANGIR P., CHAKRABORTY S., A new decomposition-based multi-objective symbiotic organism search algorithm for solving truss optimization problems, *Decision Analytics Journal*, **10**: 100371, 2024, doi: 10.1016/j.dajour.2023.100371.
26. KIM I.Y., DE WECK O.L., Adaptive weighted-sum method for bi-objective optimization: Pareto front generation, *Structural and Multidisciplinary Optimization*, **29**(2): 149–158, 2005, doi: 10.1007/s00158-004-0465-1.
27. XU B., JIN Y.J., Multiobjective dynamic topology optimization of truss with interval parameters based on interval possibility degree, *Journal of Vibration and Control*, **20**(1): 66–81, 2014, doi: 10.1177/1077546312456725.
28. CAI J., HUANG L., WU H., YIN L., Topology optimization of truss structure under load uncertainty with gradient-free proportional topology optimization method, *Structures*, **58**: 105377, 2023, doi: 10.1016/j.istruc.2023.105377.
29. BAZARAA S.M., SHERALI D.H., SHETTY C.M., *Nonlinear Programming: Theory and Algorithms*, John Wiley and Sons, 2005.
30. HILLERMEIER C., *Nonlinear Multiobjective Optimization*, Birkhäuser, Basel, 2001.
31. MARLER R., ARORA J., The weighted sum method for multi-objective optimization: New insights, *Structural and Multidisciplinary Optimization*, **41**: 853–862, 2010, doi: 10.1007/s00158-009-0460-7.
32. KLEIBER M., *Parameter Sensitivity in Nonlinear Mechanics: Theory and Finite Element Computations*, Wiley, 1997.
33. BOJCZUK D., RĘBOSZ-KURDEK A., Optimal design of bar structures with their supports in problems of stability and free vibrations, *Journal of Theoretical and Applied Mechanics*, **52**(2): 533–546, 2014.
34. BOJCZUK D., MRÓZ Z., On optimal design of supports in beam and frame structures, *Structural Optimization*, **16**(1): 47–57, 1998, doi: 10.1007/BF01213999.
35. LIN M.H., TSAI J.F., YU C.S., A review of deterministic optimization methods in engineering and management, *Mathematical Problems in Engineering*, **2012**: 756023, 2012, doi: 10.1155/2012/756023.
36. LISZKA T., ORKISZ J., The finite difference method at arbitrary irregular grids and its application in applied mechanics, *Computers and Structures*, **11**(1): 83–95, 1980, doi: 10.1016/0045-7949(80)90149-2.
37. SHI Z.-J., SHEN J., Step-size estimation for unconstrained optimization methods, *Clinics*, **24**(3): 399–416, 2005, doi: 10.1590/S1807-03022005000300005.
38. HOLLAND J.H., *Adaptation in Natural and Artificial Systems*, Cambridge, MA, USA: MIT Press, 1992.
39. BURCZYŃSKI T., ORANTEK P., Evolutionary and hybrid algorithms, [in:] Gajewski R.R. [Ed.], *Neural Networks, Genetic Algorithms, Fuzzy Sets* [in Polish], pp. 99–117, Rzeszów: BEL, 1999.

40. KOK S., SANDROCK C., Locating and characterizing the stationary points of the extended rosenbrock function, *Evolutionary Computation*, **17**: 437–53, 2009, doi: 10.1162/evco.2009.17.3.437.
41. OKASHA N., FRANGOPOL D., Lifetime-oriented multi-objective optimization of structural maintenance considering system reliability, redundancy and life-cycle cost using GA, *Structural Safety – STRUCT SAF*, **31**: 460–474, 2009, doi: 10.1016/j.strusafe.2009.06.005.
42. HUI-JUN L., ZENG-LI P., CHUN-LIANG Y., YUE-MING T., Application of advanced reliability algorithms in truss structures, *International Journal of Space Structures*, **29**: 61–70, 2014, doi: 10.1260/0266-3511.29.2.61.
43. MILEWSKI S., Recovery of thermal load parameters by means of the Monte Carlo method with fixed and meshless random walks, *Inverse Problems in Science and Engineering*, **30**(1): 1–40, 2022, doi: 10.1080/17415977.2021.2016738.
44. HUANG C., EL HAMI A., RADI B., Overview of structural reliability analysis methods – Part I: local reliability methods, *Incertitudes et fiabilité des systèmes multiphysiques*, **17-1**(Optimisation et Fiabilité): 1–10, 2017, doi: 10.21494/ISTE.OP.2017.0115.

Received December 28, 2023; accepted version April 12, 2024.

Online first May 16, 2024.



Copyright © 2024 The Author(s).
Published by IPPT PAN. This work is licensed under the Creative Commons Attribution License
CC BY 4.0 (<https://creativecommons.org/licenses/by/4.0/>).